

STUDIES OF NUCLEAR AND CYTOPLASMIC BEHAVIOUR DURING THE FIVE MITOTIC CYCLES THAT PRECEDE GASTRULATION IN *DROSOPHILA* EMBRYOGENESIS

VICTORIA E. FOE AND BRUCE M. ALBERTS

Department of Biochemistry and Biophysics, University of California at San Francisco, San Francisco, California 94143, U.S.A.

SUMMARY

Using differential interference contrast optics, combined with cinematography, we have studied the morphological changes that the living, syncytial embryo undergoes from stage 10 through 14 of *Drosophila* embryogenesis, that is just prior to and during formation of the cellular blastoderm. We have supplemented these studies with data collected from fixed, stained, whole embryos. The following information has been obtained.

The average duration of nuclear cycles 10, 11, 12 and 13 is about 9, 10, 12 and 21 min, respectively (25°C). In these four cycles, the duration of that portion of the mitotic period that lacks a discrete nuclear envelope is 3, 3, 3 and 5 min, respectively. The length of nuclear cycle 14 varies in a position-specific manner throughout the embryo, the shortest cycles being of 65 min duration.

During nuclear cycles 10 through 13, it is commonly observed in living embryos that the syncytial blastoderm nuclei enter (and leave) mitosis in one of two waves that originate nearly simultaneously from the opposite anterior and posterior poles of the embryo, and terminate in its midregion. From our preparations of quick-frozen embryos, we estimate that these mitotic waves take on average about half a minute to travel over the embryonic surface from pole to equator.

The yolk nuclei, which remain in the core of the embryo when the rest of the nuclei migrate to the periphery, divide in synchrony with the migrating nuclei at nuclear cycles 8 and 9, and just after the now peripherally located nuclei at nuclear cycle 10. After cycle 10, these yolk nuclei cease dividing and become polyploid.

The syncytial embryo has at least three distinct levels of cytoskeletal organization: structured domains of cytoplasm are organized around each blastoderm nucleus; radially directed tracks orient colchicine-sensitive saltatory transport throughout the peripheral cytoplasm; and a long-range organization of the core of the embryo makes possible coherent movements of the large inner yolk mass in concert with each nuclear cycle. This highly organized cytoplasm may be involved in providing positional information for the important process of nuclear determination that is known to occur during these stages.

INTRODUCTION

The early morphogenesis of the *Drosophila melanogaster* embryo has been extensively characterized (Rabinowitz, 1941a; Sonnenblick, 1950; Turner & Mahowald, 1976, 1977; Zalokar & Erk, 1976). The pregastrula stages, with which our study is concerned, are represented diagrammatically in Fig. 1. This figure contains our revision of a similar diagram of Zalokar & Erk (1976), in which each stage corresponds to one nuclear division cycle. After fertilization, the somatic nuclei undergo 13 consecutive, nearly synchronous nuclear divisions as a syncytium. Initially, all the

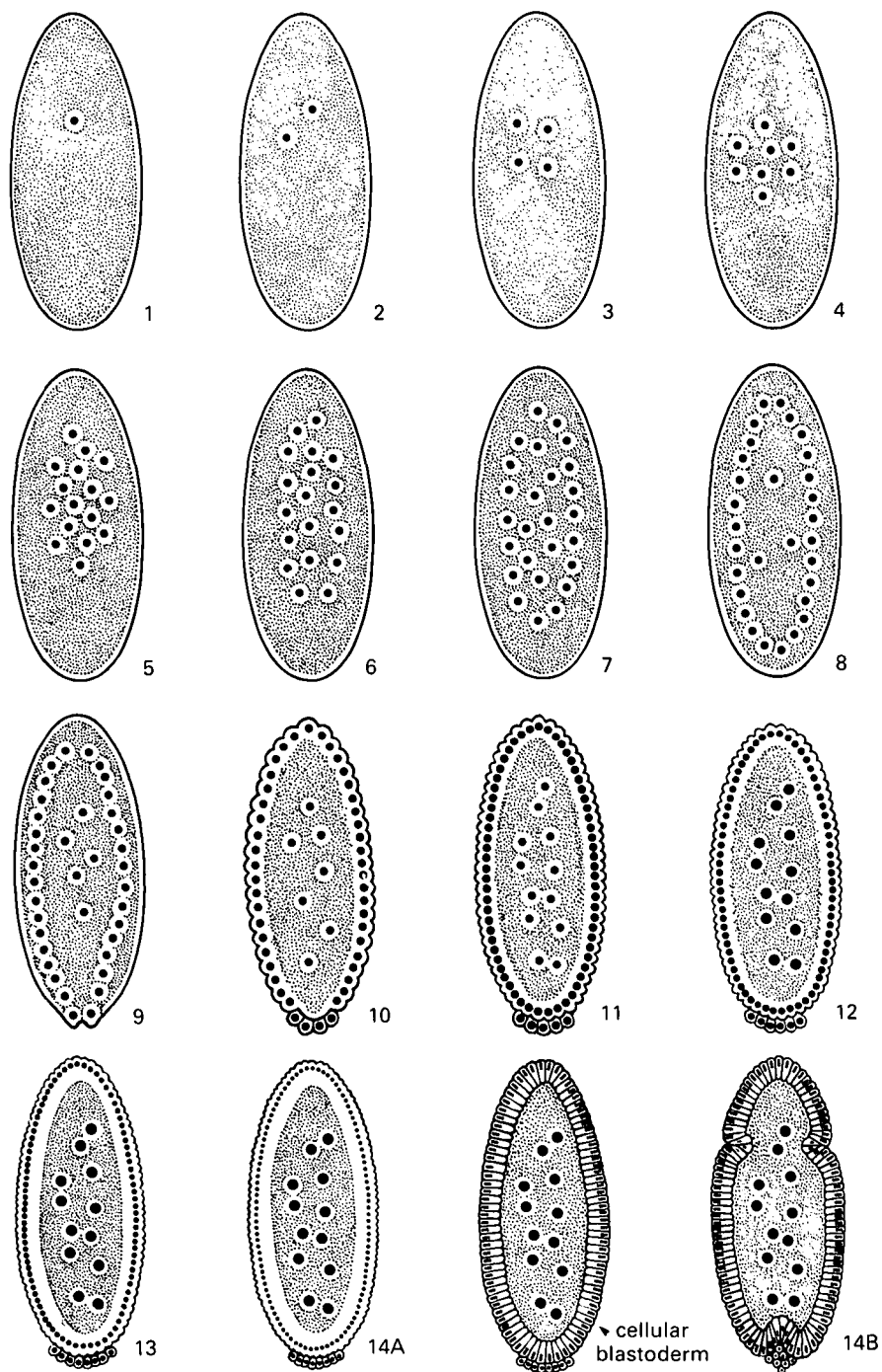


Fig. 1

Fig. 1. Schematic drawing of the embryonic stages leading up to gastrulation in *D. melanogaster*. This figure is modified from Zalokar & Erk (1976) to show the correct times of appearance of pole and somatic buds and to indicate the cessation of division of the yolk nuclei. The number beside each embryo, which denotes its developmental stage, corresponds to the total number of nuclear division cycles undergone by the almost synchronously dividing embryonic nuclei. A stage begins with the start of interphase and ends with the conclusion of mitosis. Stage 1 is the fertilized zygote during its first interphase and mitosis. The subsequent stages, each of which corresponds to one complete nuclear division cycle (interphase plus mitosis), are numbered consecutively. Embryos are shown in longitudinal section and with their anterior ends at the top. They are depicted without vitelline membranes to emphasize the changes in surface morphology of the plasma membrane that surrounds the syncytial embryo. Solid black circles represent nuclei, stippled regions denote yolk, and non-textured regions denote the yolk-free regions of cytoplasm. As shown, when development begins there is a thin layer of yolk-free cytoplasm at the egg periphery (the 'periplasm'), and a yolk-free region of cytoplasm surrounding each nucleus (the 'protoplasmic islands'). For stages 1–5 all nuclei are indicated, even though they would not all normally be in the same plane. For stages 6–14, only a fraction of the embryonic nuclei is shown.

Stages 1–7: the nuclei multiply exponentially in the central region of the egg.

Stage 8: the majority of the still dividing nuclei, with their enveloping protoplasmic islands, have started their migration outwards, leaving the future yolk nuclei behind. These yolk nuclei will divide in approximate synchrony with the remaining nuclei in cycles 8–10, and thereafter cease dividing and become polyploid (see Table 5).

Stage 9: early in their 9th interphase, a few migrating nuclei appear in the posterior periplasm, creating there the posterior cytoplasmic protuberances called pole buds. At the end of this stage, these nuclei (like all others in the syncytium) enter into mitosis, thus doubling the number of pole buds.

Stage 10: the remainder of the migrating nuclei appear in the periplasm at the beginning of their 10th interphase (see Fig. 2), organizing somatic buds over the entire embryonic surface. During mitosis of this cycle, the pole buds divide again and, nearly simultaneously, are pinched off from the syncytial embryonic mass to produce the pole cells; after this stage these cells, which are the potential germ cell progenitors, will continue to divide, but they lose mitotic synchrony with the embryonic syncytium.

Stages 10–13: the syncytial nuclei in their somatic buds at the embryonic periphery divide with near synchrony (see text). During cycle 13, the depth of yolk-free periplasm increases dramatically at the expense of the central yolk region.

Stage 14A: plasma membrane formation occurs synchronously between all of the peripheral nuclei to generate separate cells. During this process, the nuclei elongate, matching the shape of the elongated blastodermal cells that are forming. Stage 14A is depicted at both early (no cell membranes evident) and late (cellularization just completed) times. The cells that form at this time are the progenitors of the somatic tissues.

Stage 14B: immediately following cellularization, gastrulation movements begin. The infolding of cells depicted about one-third of the distance down from the anterior pole is a section of the cephalic furrow (also called the anterior oblique cleft), and the invagination at the posterior pole is part of the posterior midgut furrow (also called the amnioproctodeal invagination) into which the pole cells move. Not knowing when nuclear division occurs during stage 14, Zalokar & Erk (1976) designated the early gastrula as stage 15, rather than as stage 14B. The cells do not begin the mitosis of cycle 14 synchronously, but rather enter mitosis in a consistent region-specific sequence beginning 15 min after the start of gastrulation (see Fig. 6). Note also that a true 'cellular blastoderm' stage hardly exists in *Drosophila*, since gastrulation begins as soon as cells have formed.

The average time required for stages (nuclear cycles) 1–9 is 8 min at 25 °C (Rabinowitz, 1941a; Sonnenblick, 1965; Zalokar, 1976). Stages 10, 11, 12, 13 and 14 occupy about 9, 10, 12, 21, and more than 65 min, respectively (see Table 1; Fig. 6).

dividing nuclei are located in the interior of the egg, but by cycle 8 the majority of the nuclei have begun migrating outwards towards the egg surface leaving a small population of nuclei behind in the interior of the embryo. By cycle 9 the first nuclei to reach the surface arrive at the posterior pole of the egg. By early cycle 10, the remainder of migrating nuclei reach the egg surface and become evenly distributed in a monolayer just under it. During this same cycle, those nuclei located at the posterior pole cellularize, forming the 'pole cells', which are the potential germ cell progenitors. The remainder of the nuclei at the surface undergo four nearly synchronous divisions as a syncytium (nuclear cycles 10–13). Cellularization of these nuclei occurs during the first half of interphase 14 (stage 14A in Fig. 1), and the new cells embark on the movements of gastrulation as soon as they are formed (stage 14B in Fig. 1). The cells formed during stage 14 contain all the progenitors of the somatic tissues, including both extra-embryonic membranes and the embryonic primordium proper.

The nuclei that do not migrate to the periphery, the so-called 'yolk nuclei', become polyploid (Rabinowitz, 1941b; Poulson, 1950). These polyploid nuclei remain in the interior of the central yolk mass through the end of gastrulation. However, during germ band extension they assume positions at the surface of the yolk mass immediately underlying the developing embryonic primordium (Poulson, 1950; and our unpublished observations), remaining acellular (W. Rickoll, personal communication). The developmental significance and ultimate fate of the yolk nuclei is unknown.

The developmental fates of premigration and migrating nuclei (cycles 6–9) appear not to be determined, as assayed by ectopic transplantation of nuclei with adhering cytoplasm (Okada, Kleinman & Schneiderman, 1974). In contrast, some late syncytial blastoderm nuclei (cycle 13), when transplanted with their surrounding cytoplasm, appear to be determined for either anterior or posterior fates (Kauffman, 1980). Soon after the nuclei have become cellularized, they are further restricted in their developmental fate to specific metamer segments – as judged both by cell transplantation (Illmensee, 1978) and clonal analysis (for a review, see Lawrence, 1981). Experiments in which *Drosophila* embryos are ligated after various times of development suggest that the spatial patterning that makes possible this specification of segmentation is created in a gradual fashion prior to cellularization – the most distal segments (i.e. the most anterior and most posterior segments) being elaborated first, with more central segments patterned subsequently (Schubiger, Mosley & Wood, 1977; Vogel, 1977) (for a comprehensive review of insect segment determination, see Sander, 1976, 1981).

A little nuclear RNA synthesis can be detected before nuclear migration. During nuclear cycles 10 through 13, increased RNA synthesis occurs in both the somatic and yolk nuclei. There is a striking increase in the rate of this nuclear RNA synthesis early in cycle 14, as cell membranes begin to form around the somatic nuclei (Lamb & Laird, 1976; McKnight & Miller, 1976; Zalokar, 1976; Sinha & Pellegrini, 1982).

It is clear from this brief review that nuclear cycles 10 through 14 represent a critical period for the developing *Drosophila* embryo. This paper reports our cytological studies of the embryo during the five nuclear cycles that lead to the formation of the first determined somatic cells.

MATERIALS AND METHODS

Egg collection and staging

Population cages of laying *D. melanogaster* (Oregon R) flies were maintained and their eggs harvested essentially as described by Elgin & Miller (1978). Eggs harvested after 1–3 h collections were freed from their chorions ('dechorionated') by immersion and gentle swirling in a 50% solution of Chlorox (active ingredient sodium hypochlorite) for 90 s, followed by extensive rinsing. The rinse solution (used also to flush eggs from collection plates) was 0·4% NaCl, 0·03% Triton X-100. To select embryos of the approximate age desired, batches of dechorionated embryos immersed in rinse solution were viewed with a dissecting microscope using transmitted light (50 \times). Both the first appearance of pole buds (marking 1 min after the start of nuclear cycle 9) and the first appearance about 9 min later of the somatic buds at the anterior tip of the embryo (marking 1 min after the start of cycle 10) can be clearly seen with these optics (these two stages are shown with other optics in Fig. 3). After preliminary staging, selected embryos were transferred by pipetting to slides in preparation for higher magnification viewing, and the timing was begun with the next appearance of somatic buds at the anterior tip of the embryo. During nuclear cycles 11–14, the appearance of new buds signal the entrance into each interphase (see text). The somatic buds appear suddenly, and we find that the accuracy of staging embryos in this way is $\pm 1\cdot0$ min per cycle at 25 °C (see Table 1). The observed cycle times were the same whether the embryos were immersed in Halocarbon oil (see below) or in the aqueous rinse solution.

Microscopy of living embryos

Zeiss Nomarski Differential Interference Contrast (DIC) optics (with the DIC prism in the focal plane of the objective) were used in most cases. For many studies, embryos were immersed in the 0·4% NaCl, 0·03% Triton X-100 rinse solution and observed uncovered on a ring slide using a Plan-Neofluor 25/0·8 oil, glycerol, water-immersion objective. Alternatively, either the same objective or a Planapochromat 63/1·4 oil-immersion objective was used with covered preparations. For these preparations, an embryo was placed on a slide, rinsed with a gentle stream of 95% ethanol, air dried for 1–2 min, and covered with a drop of Halocarbon oil (series 11–21 Halocarbon Products Corporation, 82 Burlews Court, Hackensack, New Jersey). A no. 1 coverslip was placed on each side of the oriented embryo, and a third coverslip was positioned over the embryo such that this glass was supported by the pair of no. 1 coverslips; the sides were left unsealed to allow oxygen exchange. Single embryos in both our uncovered and covered preparations develop normally until hatching (described as 'viable embryos' in the text). Oxygen deprivation (which can arise in sealed or overcrowded preparations) leads to severe perturbations in the nuclear cycle, developmental arrest and abnormalities (Foe, unpublished data) and was therefore avoided.

For oil-mounted preparations, the temperature of the slide was maintained at 25 \pm 0·5 deg. C with an airstream stage incubator (Nicolson Precision Instruments Inc., model C300). Other studies were carried out at room temperature, which varied between 22 °C and 25 °C. The film used for both DIC and fluorescence photography was Kodak Pan 2415.

Time-lapse video cinematography

Video-taping was carried out through the phototube of the microscope using the Zeiss DIC optical system described above for high-resolution studies. When less resolution but higher contrast was preferable, as for the studies summarized in Figs 10 and 13, phase or simple transmitted light optics were used instead. A TV camera (RCA model TC 1005/no. 1), interphased with a time-lapse video recorder (Panasonic VTR model NV-8030) and a time and date generator (Panasonic model WJ-800), were used for the recordings. Yolk contractions were studied at recording speeds of 72 \times and 36 \times at magnifications of 500–2000 \times ; saltatory movements were examined both at a recording speed of 9 \times and in real time, at a magnification of 4000 \times .

Preparation of fixed whole embryos for fluorescence microscopy

In most cases, embryos were mass-prepared using a protocol introduced by T. Mitchison & J. Sedat (unpublished results). Dechorionated embryos (0·1–1·5 g) were extensively rinsed in the

NaCl/Triton solution and then transferred into modified buffer A, which we shall designate as buffer AM (Burgoyne, Wagar & Atkinson, 1970: 80 mM-KCl, 20 mM-NaCl, 2 mM-Na₃EDTA, 0.5 mM-Na₃EGTA, 0.5 mM-spermidine·HCl, 0.2 mM-spermine·HCl, 0.1% β-mercaptoethanol, 15 mM-PIPES (piperazine-N-N'-bis(2-ethanesulphonic acid), adjusted to pH 7.4). The change in buffer was accomplished by allowing the embryos to settle out of the NaCl/Triton solution in a 20 ml test tube and resuspending them directly in buffer AM. As in all handling of embryos, the embryos were resuspended as soon as they had settled in order to avoid the anoxia caused by overcrowding. The embryos in buffer AM were then left to settle again and resuspended in a mixture of 5 ml buffer AM, 5 ml heptane (Baker reagent), and 0.6 ml freshly boiled 37% formaldehyde. Embryos were shaken vigorously for 10 min at room temperature in this two-phase permeabilization and fixation medium (in a manner analogous to that of Limbourg & Zalokar, 1973), collected on a stainless steel filter, and then plunged into a mixture of 10 ml heptane and 10 ml 90% methanol, 50 mM-Na₃EGTA that had been precooled to -70°C. The frozen embryos were agitated vigorously in a flask at -70°C for 10 min and then warmed rapidly to room temperature by vigorously swirling the flask under a stream of hot tap water. After warming, the swirling was continued another 2–5 min or until about 90% of the embryos were free of their ruptured vitelline membranes. The devitellinized embryos sink to the bottom of the lower methanol phase, while free vitelline membranes and embryos still enveloped in this membrane remain at the methanol-heptane interphase. The membrane-free embryos were removed by pipette, rinsed twice with 5 ml of 90% methanol, 50 mM-Na₃EGTA, and then rehydrated successively through two 5 ml changes each of 70%, 50% and 25%, methanol/EGTA solutions (in which the added aqueous component is buffer AM). The embryos were rinsed twice in buffer AM, stained for 4 min in buffer AM containing 1 µg/ml of the fluorescent, DNA-specific dye Hoechst 33258 (American Hoechst Corp.), and rinsed a final time in buffer AM. The embryos were then cleared by stepwise transfer through a series (0.5 ml each) of 25%, 50% and 100% glycerol (Baker 'phototrex' grade diluted with buffer AM). In all cases, the exchange time allowed was that required for the embryos to settle to the bottom of the tube containing the exchange medium.

The above protocol was modified in order to determine whether mitotic waves occur in embryos that have not been exposed to dechorionating solutions. In these experiments, embryos were rinsed from the collection plate directly onto a screen that was plunged immediately into the -70°C mixture of heptane/methanol/EGTA. The remainder of the normal protocol was then followed except that, after warming, vigorous swirling was continued for 10 rather than for 2 to 5 min. Both devitellinized embryos (~40% of the starting material) and embryos inside intact chorion and vitelline membranes sink to the bottom of the methanol phase; however, a large percentage of the latter embryos was removed when the mixed population of embryos was transferred into 25% glycerol, since they sink more slowly than devitellinized embryos. The morphology of the embryos treated according to this modified protocol is inferior to that of embryos treated according to the original procedure; the morphology was however adequate for obtaining the mitotic wave data described in Table 3.

The fluorescently stained embryos in 100% glycerol were transferred to slides and overlaid with coverslips for viewing. We used a Zeiss Epi-illumination system with the Zeiss 01 filter set (excitation beam of 365 nm split with a dichroic mirror at 420 nm, plus a LP-410 nm barrier filter), together with a Neofluor 100/1.25 or a Plan-Neofluor 25/0.8 oil, glycerol, water-immersion objective.

Fixed embryos were staged by their number of surface nuclei per unit area, measured using a 5 mm × 5 mm eye piece graticle. Cycle 10, 11, 12, 13 and 14 embryos have 4–6, 7–10, 12–19, 27–44 and 60–84 nuclei per 2200 µm², respectively. The variation in nuclear counts is less across one embryo than between different embryos at the same stage, and is apparently mostly due to differences in the size of embryos in the population.

Microinjection into living embryos

Prestaged, dechorionated embryos were placed on a slide, rinsed gently with a stream of 95% ethanol, and desiccated over CaCl₂ for 6–10 min. Embryos were then covered with Halocarbon oil and microinjected with the desired inhibitor concentration. We determined the volume injected to be approximately 2 × 10⁻⁴ µl or 1–3% of the average *Drosophila* embryo volume of 1.5 × 10⁻² µl (Okada, Komatsu & Okumura, 1980). Intracellular concentrations are given on the assumption that the inhibitors spread evenly within the embryos. The concentrated cytochalasin (Merck)

and colchicine (Sigma) solutions for injections were made up in dimethylsulphoxide and in water, respectively. Injections were performed using a Leitz micromanipulator with injection needles of about 3 μm diameter pulled from 1 mm diameter, glass-fibre extruded capillary tubing that had been acid-washed and siliconized. Time-lapse video recordings were made of the development of each injected embryo as described above.

Visualization of the yolk fibres

When an embryo is squashed into buffer AM that contains 10 $\mu\text{g}/\text{ml}$ Hoechst dye 33258 (with or without 1 % formaldehyde), many long fibres are released which stain faintly with the dye. These fibres are also visible under DIC or darkfield optics. However, we find that the fibres are most clearly seen when the embryo is squashed into buffer AM containing 2 $\mu\text{g}/\text{ml}$ rhodamine B isothiocyanate (RITCB from Sigma; unpublished observations of T. Karr in this laboratory). The RITCB adsorbs to the fibres, allowing them to be visualized by fluorescence microscopy with the Zeiss 15 filter set. In all of these preparations, the fibres are best displayed when the squashed material is partially dispersed by the flow caused by blotting from an edge of the coverslip.

RESULTS

The nuclei migrate outwards in a stepwise manner during cycles 7 to 10

In order to determine precisely when the migrating cycle 10 nuclei arrive at the embryo surface, we have followed the migration of the nuclei by analysing data from a large number of fixed and stained embryos of mixed ages.

In Fig. 2, the average distance of the somatic nuclei from the embryo surface is plotted as a function of the nuclear cycle phase in stage 8 to 10 embryos. Note that most, if not all, of the outward nuclear movement occurs during one brief period in each division cycle, corresponding to telophase and very early interphase. During this brief period, the nuclei must move at a rate of 10–15 μm per min. Our analysis also reveals that about 10 % of all of the cycle 10 embryos contain nuclei that are still migrating and that these nuclei have morphologies characteristic of very early interphase (Foe, unpublished data). The nuclei in the remaining cycle 10 embryos have reached their final position about 2.5 μm from the embryo surface. Since cycle 10 lasts for a total of 9 min (see below), we conclude that the nuclei complete their outward migration after about 1 min of cycle 10 has elapsed.

Beginning with cycle 9, each nuclear cycle produces a cycle of cytoplasmic budding on the embryo surface

At about 80 min post-fertilization, during what we infer to be nuclear cycle 9 (Zalokar & Erk, 1976; Turner & Mahowald, 1976), the future pole cell nuclei, having reached the posterior surface of the *D. melanogaster* egg, create there the cytoplasmic protuberances known as 'pole buds'. During the next few minutes, these pole buds (initially 1–5 in number) increase in size, and divide once. Both the pole buds and the nuclei within them are readily visualized in living embryos by DIC microscopy, as exemplified in Fig. 3.

Similar, though slightly less protruding, 'somatic buds' are formed over the entire egg (Ede & Counce, 1956; Turner & Mahowald, 1976; Warn & Magrath, 1982) when the somatic nuclei appear at the surface about 9 min after the initial appearance of the

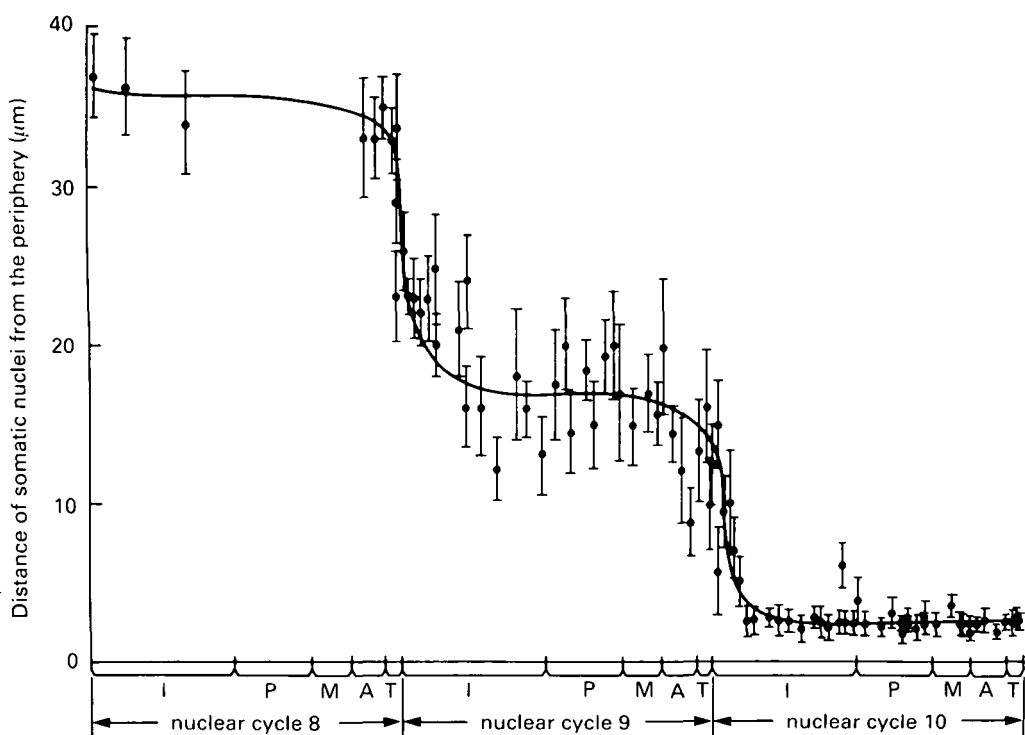


Fig. 2. The stepwise, outward migration of the somatic nuclei that gives rise to the syncytial blastoderm. These data were collected by analysis of embryos that were fixed and stained with the DNA-specific dye Hoechst 33258, using the original protocol of Mitchison & Sedat (see Materials and Methods). The cycle 10–14 embryos were staged by the number of their surface nuclei per unit area (see Materials and Methods), while cycle 9 embryos were distinguished from cycle 8 embryos by the presence of pole buds. In each case, the precise phase within each cycle was determined by nuclear diameter and the chromosome morphology of the fluorescently stained nuclei (Foe, unpublished). The distances reported are those of the closest approach of the nuclear envelope to the embryo surface, as measured with an eyepiece micrometer in an optical midsection of the embryo (such as displayed in Fig. 11A). Each point on the graph represents the average of measurements on eight nuclei in a single embryo, with the bars indicating the standard deviation. All cycle 10 embryos whose nuclei displayed a morphology and nuclear diameter characteristic of early interphase (diameter less than 7 μm ; Foe, unpublished) had their somatic nuclei at distances greater than the final 2.5 μm from their periphery. Complete data for cycle 7 and 8 embryos were not collected; our preliminary data indicate that nuclear migration begins at telophase of cycle 7. I, interphase; P, prophase; M, metaphase; A, anaphase; T, telophase.

Fig. 3. Chronological DIC micrographs of a living embryo showing the appearance of pole buds and somatic buds. In this and in all subsequent micrographs and drawings (except Fig. 4) the embryo anterior is towards the left, and the dorsal surface toward the top of the page. The numbers on each micrograph represent developmental age in min (25 °C), where zero time is arbitrarily set at the moment of the first detectable protrusion of the somatic buds at the anterior of the embryo; this corresponds to about 1 min after the entrance of the anterior nuclei into interphase 10 (see legend to Table 1). At the time designated as -9.0 min (end of cycle 8), neither somatic buds nor pole buds have formed. By -4.0 min (mid-cycle 9), the pole buds (*pb*) are present but the somatic buds have not yet appeared. By 4.0 min (mid-cycle 10), the somatic buds (*sb*) have appeared, and cellularization has resulted in the transformation of the pole buds into pole cells (*pc*). See Fig. 4 for a higher magnification view of somatic budding. $\times 380$.

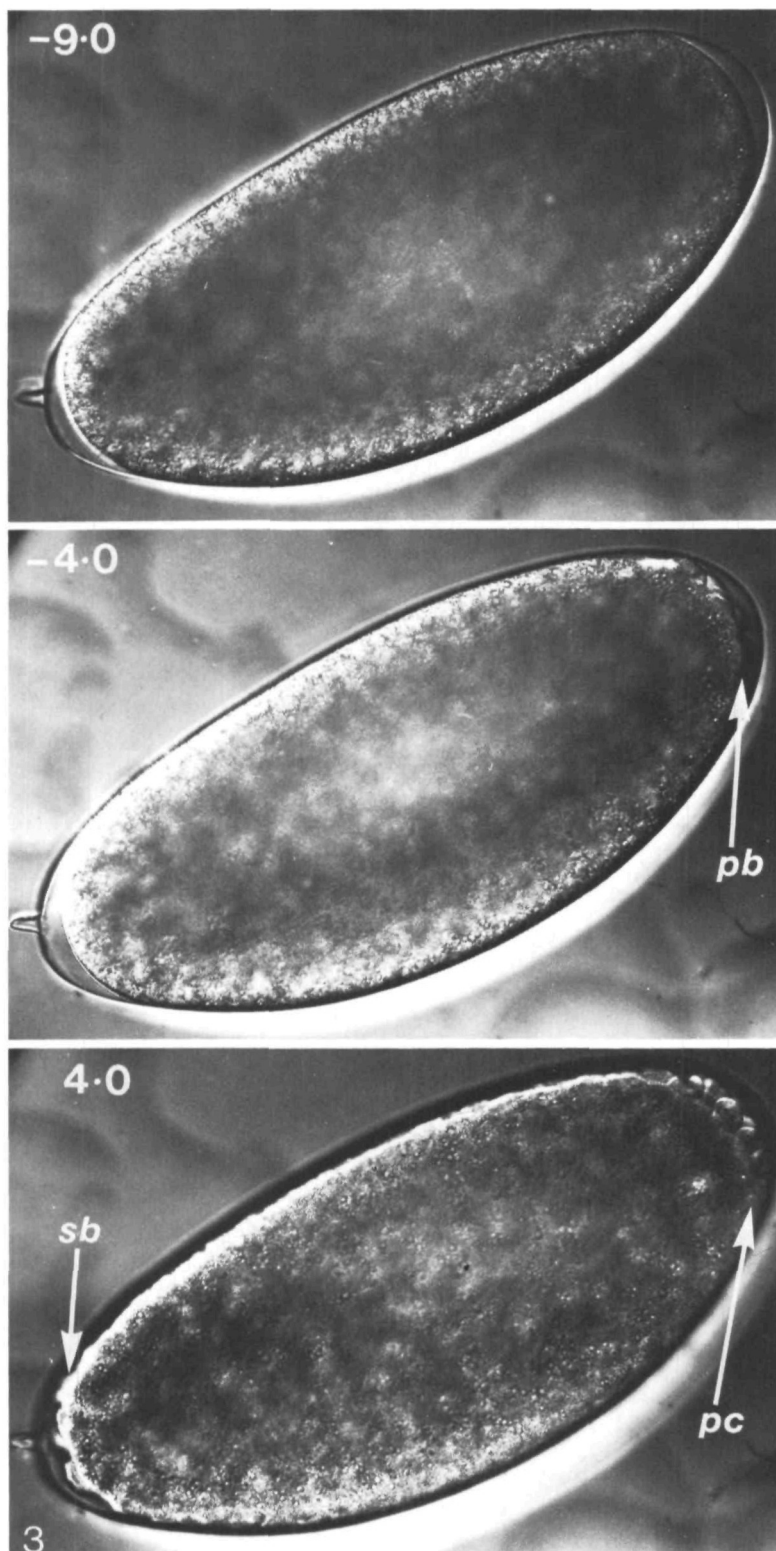


Fig. 3

pole buds. The somatic buds make their first appearance at about 1 min into interphase of nuclear cycle 10, at precisely the same time that the somatic nuclei complete their migration to the embryo surface (see Fig. 2).

In live embryos, the somatic buds are most conveniently observed at the anterior end of the embryo, since a gap normally exists there between the embryo plasma membrane and the vitelline membrane, which allows the buds to protrude without distortion (Fig. 4). However, somatic buds and their nuclei are also visible on the remaining embryo surface, where the buds are compressed against the vitelline membrane (Fig. 5). Continuous observation of living embryos reveals a cyclic appearance and disappearance of both the somatic buds and the nuclei within them (Figs 4, 5). A bud first appears as a small rounded bulge in the plasma membrane, and subsequently increases in volume and extent of protrusion. This increase in bud size coincides with a large increase in nuclear volume that occurs during each interphase (Fig. 4; Foe, unpublished). The bud subsequently collapses into an irregular form as the nucleus enters mitosis and the nuclear boundary becomes indistinct. After a few minutes a new budding cycle begins, as two new cytoplasmic buds appear where one had been, each with a distinct round nucleus (Fig. 4). The cycle of somatic bud formation and collapse occurs four times, defining nuclear cycles 10 through 13. After a fifth cycle of bud formation (the start of nuclear cycle 14), cleavage furrows begin to form synchronously between adjacent buds; this furrowing process results in the cellularization of each of the blastoderm nuclei prior to their next nuclear division.

As a convenient measure of the time that elapses between each nuclear division, the successive budding cycles were timed at the anterior tip of 20 embryos. The times during which the nuclear contours were indistinct were also noted. These data for living embryos are displayed in Table 1. The average durations thereby determined for cycles 10, 11, 12 and 13 are about 9, 10, 12 and 21 min, respectively, at 25°C. In these same cycles there were 3, 3, 3 and 5 min of elapsed time during which no distinct nucleus was visible. Comparison with our studies of fluorescently stained, whole embryos, presented in Table 2, suggests that this 3 min period in cycle 10 includes not only the portion of the mitotic phase of the cycle in which the nuclear envelope is completely disrupted, but also part of a period during which the nuclear envelope appears to be partially formed in fixed embryos (Foe, unpublished data).

A greater amount of time is required for cycle 14. During the first 50 min of cycle

Fig. 4. One complete cycle of nuclear division and somatic bud formation as seen with DIC optics at the anterior tip of a living embryo. The number on each micrograph represents the chronological age, determined as for Fig. 3. First, the nucleus and its enveloping cytoplasmic bud swell during early interphase of cycle 10 (0–3·0 min). The breakdown of the bud and nucleus during mitosis of cycle 10 is next seen (4·5–6·5 min). Finally, new buds make their appearance and then swell during interphase of cycle 11 (8·3–10·3 min). The cytoplasmic flow (see text) results in back-and-forth movements of the buds relative to the rigid vitelline membrane; hence, in order to keep the buds in view, different focal planes were required for these sequential micrographs.

The fibrous nature of the peripheral cytoplasm, with fibres running perpendicular to the embryonic surface, can be faintly discerned in these micrographs (e.g., see arrows in 8·3 min panel). $\times 640$.

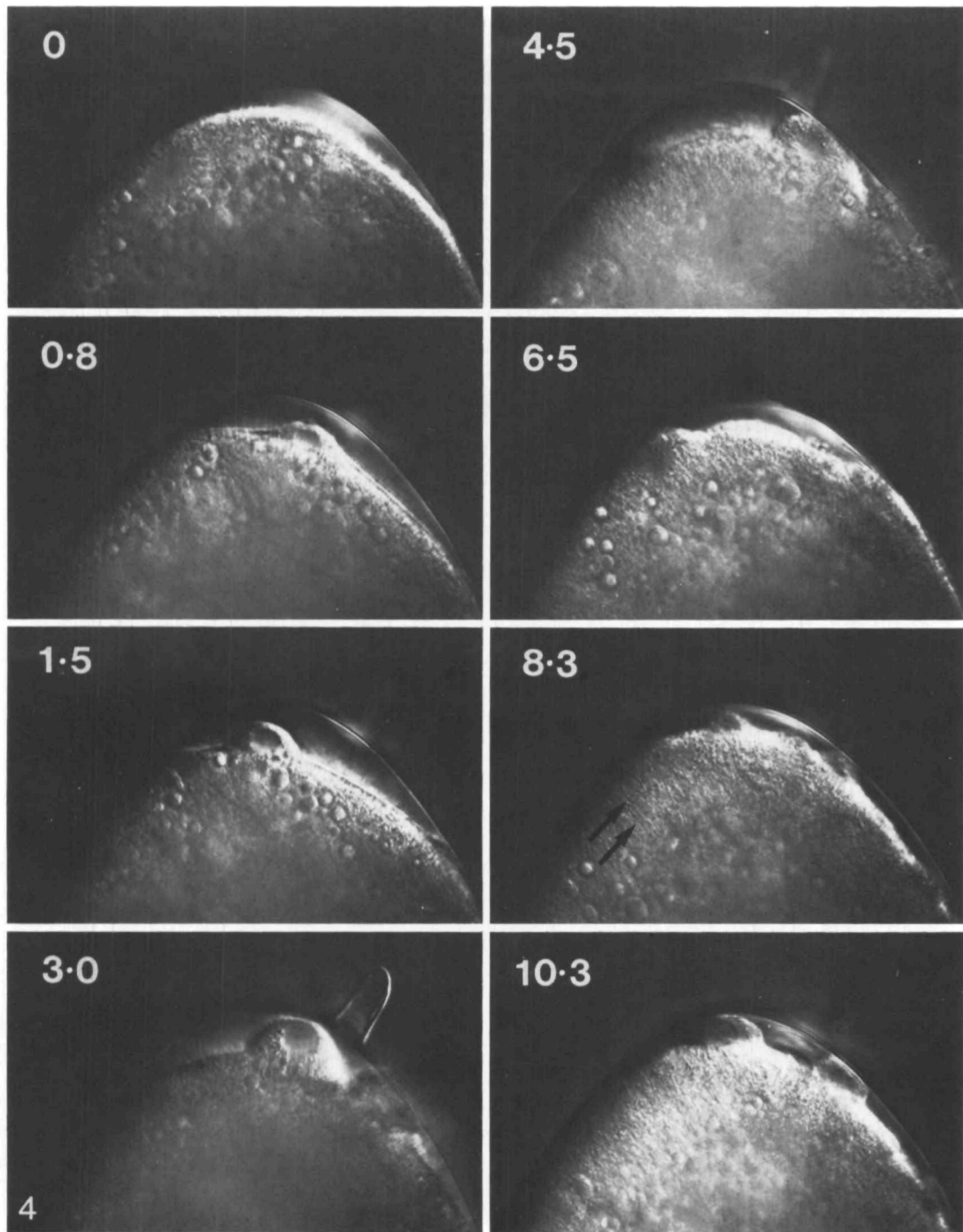


Fig. 4

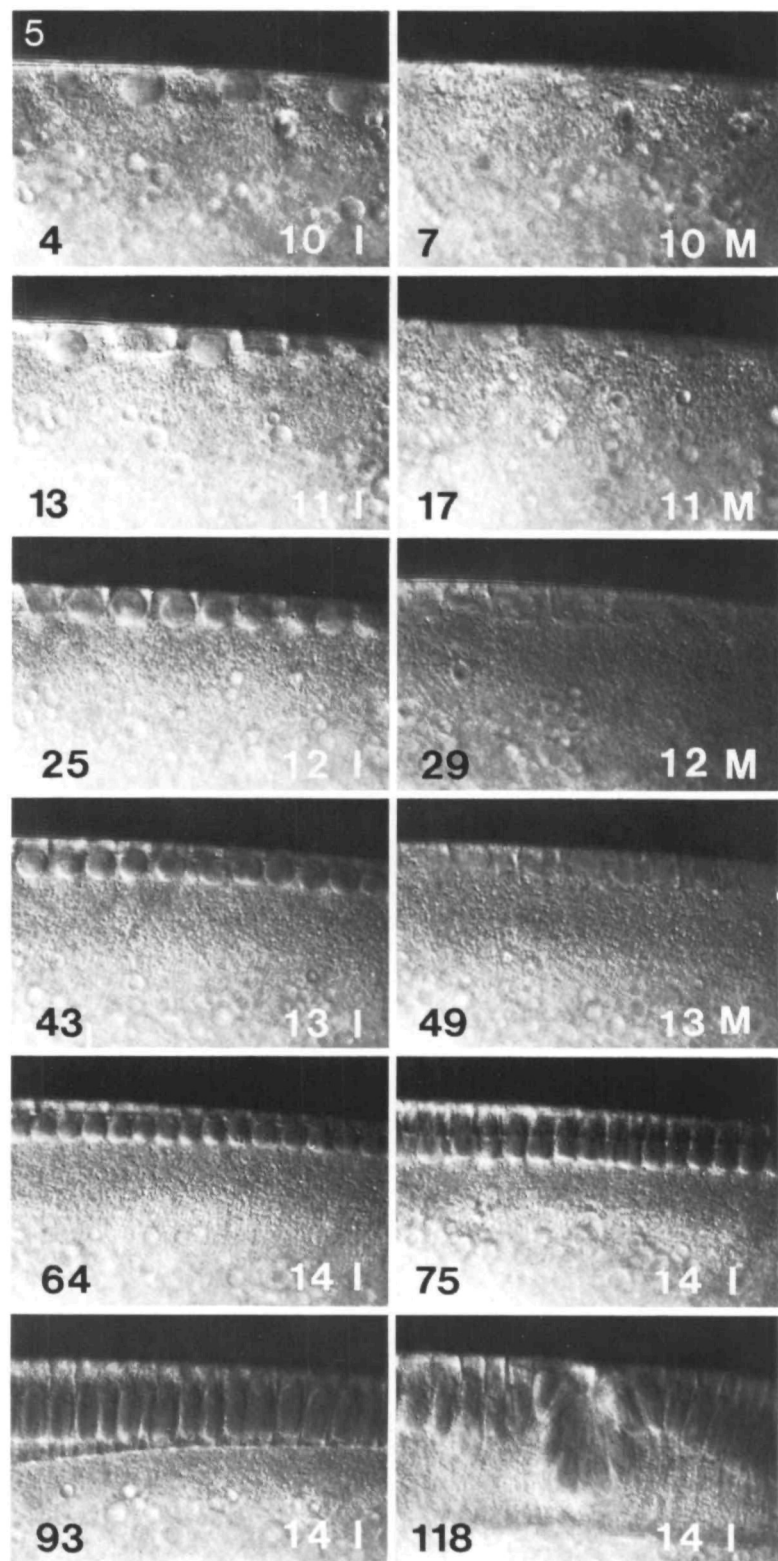


Fig. 5

Table 1. Nuclear cycle times determined from observation of live embryos

Developmental stage	Total length of budding cycle*	Duration (min at 25 °C)	
			Portion of budding cycle lacking a distinct nuclear envelope
10	7.8 ± 0.6 (N = 19)†		3.3 ± 0.9 (N = 10)
11	9.5 ± 0.7 (N = 20)		3.0 ± 0.9 (N = 10)
12	12.4 ± 0.9 (N = 18)		3.3 ± 0.9 (N = 13)
13	21.1 ± 1.5 (N = 17)		5.1 ± 0.9 (N = 16)

* The length of each budding cycle corresponds to the length of each nuclear cycle for all cycles except cycle 10. For cycle 10 only, there is a delay of about 1 min between the start of interphase and the initiation of budding, due to the fact that the outward nuclear migration is not yet complete when cycle 10 begins (see Fig. 2). Thus, the true length of cycle 10 is about 8.8 min (i.e., 7.8 + 1 min).

† The N values denote the number of embryos on which observations were made. Data were collected by analysis of chronological photographs of 20 embryos, but not all embryos could be scored for all determinations.

14 (at 25 °C), cleavage furrows form by the inward growth of the plasma membrane (Fig. 5). At 50 min, very close to the time that cellularization is complete, gastrulation movements begin. Thereafter, cell movements, invaginations and shape changes make it difficult to follow the behaviour of specific nuclei *in vivo* using DIC optics. However, examination of fixed and stained gastrulae reveal that the first cells enter mitosis during an early stage of germ-band elongation, which occurs about 65 min after the start of cycle 14 (as judged by comparison of the morphology of fixed embryos with the developmental sequence determined from living embryos). Instead of appearing uniformly across the gastrula at this time, cells are found to enter mitosis in a highly reproducible, region-specific sequence, as detailed in Fig. 6. Thus, the

Fig. 5. Somatic nuclei during cycles 10–14. These nuclei, which were photographed with DIC optics, were located about one-third of the distance from the anterior end (embryo anterior is towards the left), in the region of eventual cephalic furrow formation. The micrographs are all of the same embryo. The black number in the bottom left corner of each micrograph designates the chronological developmental age, determined as described in Fig. 3. The white number in the lower right corner of each micrograph designates the nuclear cycle number, with the letters I and M standing for interphase and mitosis, respectively. Nuclei are clearly discernable during interphase, but their contours become indistinct during mitosis.

Note that the somatic buds in this mid-region of the embryo, being constrained by the vitelline membrane, do not protrude as conspicuously as they do at the poles (compare with Fig. 4). Instead, the buds are pressed down against each other, creating an apparent infolding of the plasma membrane between adjacent nuclei (e.g., see panels 11 I and 12 I, above).

The first three micrographs that are marked 14 I illustrate the changes in nuclear shape that occur during the progressive inward growth of the new plasma membranes throughout interphase of nuclear cycle 14. The final panel in this sequence illustrates cephalic furrow formation, one of the first of the gastrulation movements undergone by cycle 14 nuclei. ×672.

Table 2. Duration of the various phases in the nuclear cycle, as determined by analysis of both fixed and live *Drosophila* embryos at cycle 10

	Interval with visible nuclear envelope			Interval with disrupted nuclear envelope			Metaphase	Anaphase	Telophase	Total
	Interphase	Prophase	Prometaphase	Total	7	6				
Number of fixed embryos observed	27	3	11	41	7	6	3	16		
Proportion of total fixed embryos (%)	47	5	19	72	12	11	5	28		
Estimated duration (min), based on a complete nuclear cycle time of 8.8 min	4.1	0.4	1.7	6.3	1.1	1.0	0.4	2.5		
Duration (min), observed in live embryos	—	—	—	5.5	—	—	—	—	3.3	

The data on fixed embryos were derived from analysis of a 0–2.5 h collection of embryos, which had been fixed and stained with Hoechst 33258 according to the original procedure of Mitchison & Sedat (see Materials and Methods). A random sample of these fixed embryos was placed on a slide and the cycle 10 embryos were selected by their characteristic number of nuclei per unit area (see Materials and Methods). Data on all of the cycle 10 embryos present on 5 slides are presented. The phase of the nuclei in each of these embryos was determined by nuclear diameter and chromosome morphology (Foe, unpublished). Some embryos were observed with nuclei distributed between two phases of the division cycle (see Table 3, below); for each of these embryos, 0.5 embryo was assigned to each of these two phases. Nuclei showing condensed chromosomes aligned on a spindle are designated as in metaphase if no nuclear envelope is visible. Similar metaphase chromosome arrangements with visible nuclear outlines are seen, and these are designated as in prometaphase. For the live embryos, the interval during which cycle 10 nuclei displayed a visible nuclear envelope was determined by DIC optics (see Table 1, and text).

total duration of cycle 14 varies for different nuclei, but is at least 65 min long.

The behaviour of the somatic buds suggests that there is a structured region of cytoplasm around each nucleus, which divides every time that the nucleus divides. In each successive budding cycle there is less cytoplasm per bud, and the somatic buds are correspondingly smaller (see also fig. 11 of Turner & Mahowald, 1976). During cycles 10 through 13, these buds are seen by time-lapse photography to move as coherent units back and forth along the embryo surface (see legend to Fig. 4), as part of the cytoplasmic flows that move the nuclei (see text and Fig. 9 below).

Mitosis occurs in waves

It has been reported that the nuclear divisions in the syncytial blastoderm embryo (cycles 10 through 13) are synchronous (Zalokar & Erk, 1976; Sonnenblick, 1950). However, our careful observation of living embryos with DIC optics reveals that most, if not all, of the nuclear divisions occur metachronously rather than synchronously;

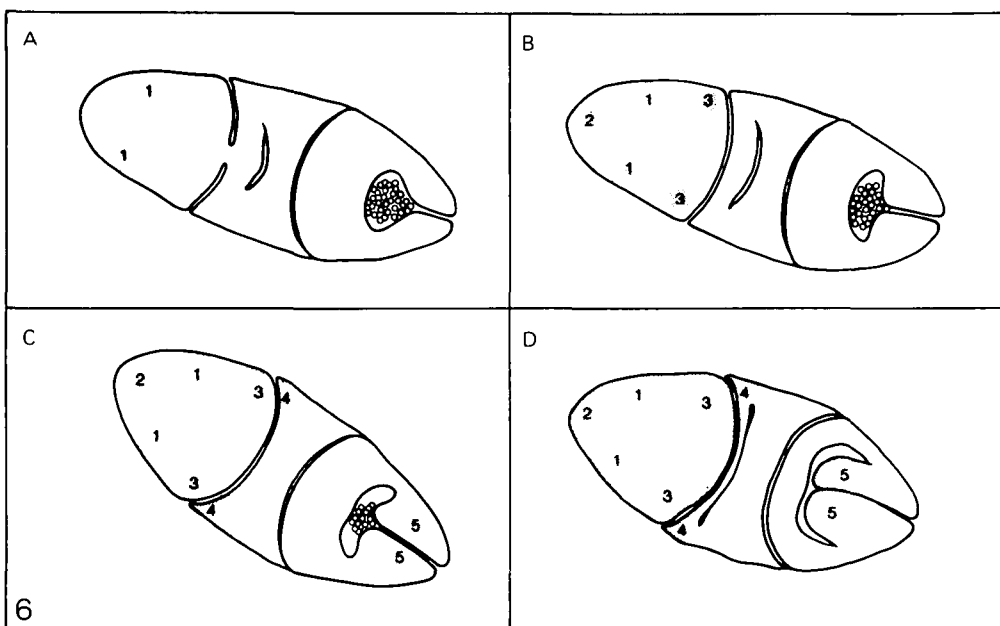


Fig. 6. The patterned sequence in which somatic nuclei enter the mitosis that ends cycle 14. Panels designated A, B, C and D are drawings of the dorsal surface of embryos during sequential stages of early germ-band elongation. The regions where cells have passed out of interphase 14 are denoted by stippling, and are numbered in the temporal order in which each group of cells first enters mitosis. The first patch of cycle 14 mitotic cells to appear are those shown in A. Only about 8 min of developmental time separate the stage shown in A from that shown in D. Patches of mitotic cells first appear on the ventral surface at the stage depicted in B; in E and F we present fluorescence micrographs of the mitotic patterns in fixed, Hoechst 33258-stained embryos at this time, with the ventral surface displayed in E and the dorsal surface in F. These embryos have been flattened somewhat to increase the area in focus ($\times 342$). The pronounced bilateral symmetry of the mitotic patterns is maintained during later stages of germ-band elongation, as cells in other regions of the embryo enter their 14th mitosis.

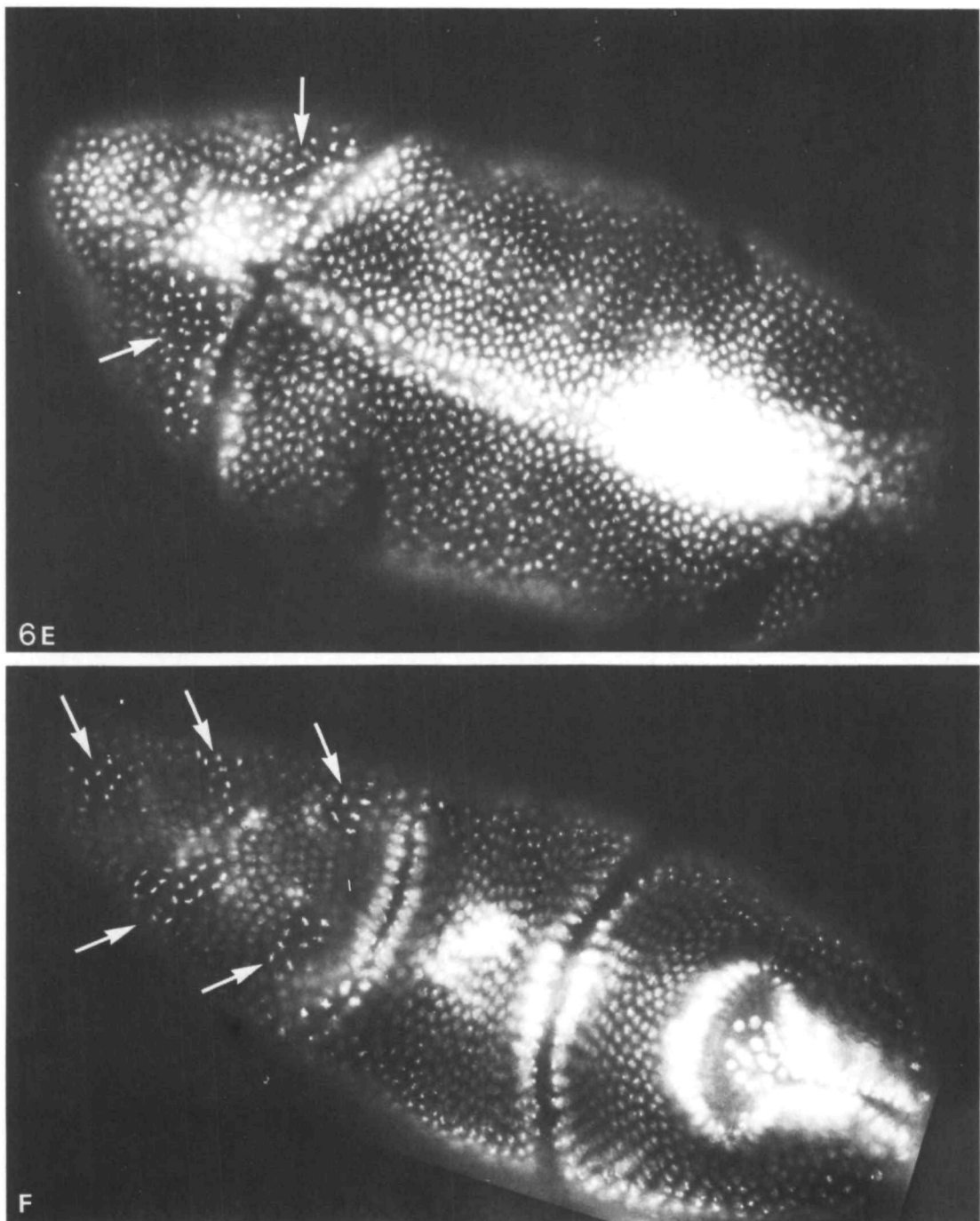


Fig. 6E–F. For legend see p. 45.

that is, entrance into (and exit from) cycles 10, 11, 12 and 13 progresses as a wavefront through the embryonic nuclei, with the nuclei behind the front being arranged in a shallow gradient of mitotic stages. These 'mitotic waves' usually originate from two separate sites, one near the anterior and the other near the posterior pole of the embryo, and progress from these two sites across the embryonic surface to meet near the equator of the embryo. Thus the nuclei near the equator are the last to enter (and the last to leave) mitosis during each cycle. In Fig. 7, we present DIC micrographs of a typical living embryo illustrating a wave-like entrance into and exit from the mitosis that concludes nuclear cycle 13.

Studies of living, dechorionated embryos during stages 12 through 14 reveal that there is considerable heterogeneity among embryos in the following respects. (1) The speed of the observed waves varies, ranging from 50 to greater than 250 $\mu\text{m}/\text{min}$ (the speed of the faster waves is difficult to measure in live embryos). (2) Although the anterior and posterior waves usually begin nearly simultaneously, frequently the wave from one pole begins as much as 2 min before that from the opposite pole. It is striking that in this case the wave that begins first stops near the equator of the embryo. (3) The site from which the mitotic waves originate, though near the poles, is not precisely the same in all embryos. However, both the speed of the waves and their sites of origin tend to remain constant between cycles for any given embryo.

We have reproducibly observed mitotic waves in living embryos whether they are immersed in the aqueous rinse solution or in Halocarbon oil. However, to test the possibility that the mitotic waves could be induced by some other aspect of our preparative technique (for example, by the Chlorox treatment used for chorion removal), we have examined freshly collected, untreated embryos whose development was stopped instantaneously by plunging them directly into a heptane/methanol mixture at -70°C (see Materials and Methods). These embryos were stained with the DNA-specific dye Hoechst 33258, so that mitotic patterns over the entire embryo surface could be observed by fluorescence microscopy. Data from 101 embryos in mitosis of cycles 10 through 12 are compiled in Table 3. Because the morphological transitions from metaphase to anaphase and from anaphase to telophase are more readily distinguished than other transitions, indexing for waves was done only on these two transitions. It can be seen from Table 3 that there were many embryos that contained nuclei in two distinct phases of mitosis. In these embryos the nuclei near one or both poles were more advanced than the nuclei in the equatorial region, as expected from our study of living embryos. From the frequency with which embryos contained waves of nuclei in the most clearly detected transition – that from metaphase to anaphase – we estimate that an average mitotic wave requires no more than 0.5 min to traverse from a pole to the equator (Table 3). A fixed embryo with the typically observed mitotic wave pattern is shown in Fig. 8.

We believe that our quantitation of rapid mitotic waves in *Drosophila* embryos resolves a longstanding controversy arising from studies of fixed embryos. Early studies showed gradients of nuclear cycle phases (Huettner, 1933; Rabinowitz, 1941a; Sonnenblick, 1950), but these were interpreted as resulting from the slow penetration of fixative through the punctured egg membranes (it took up to 5 min for

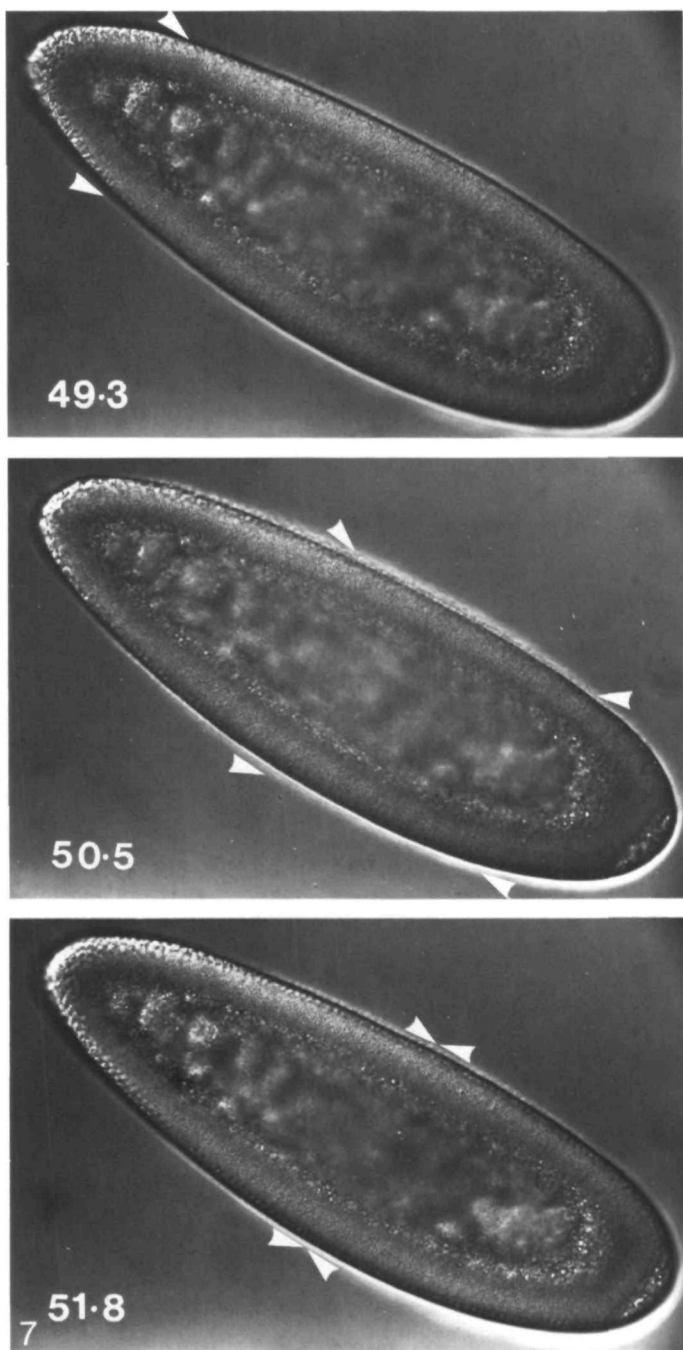


Fig. 7

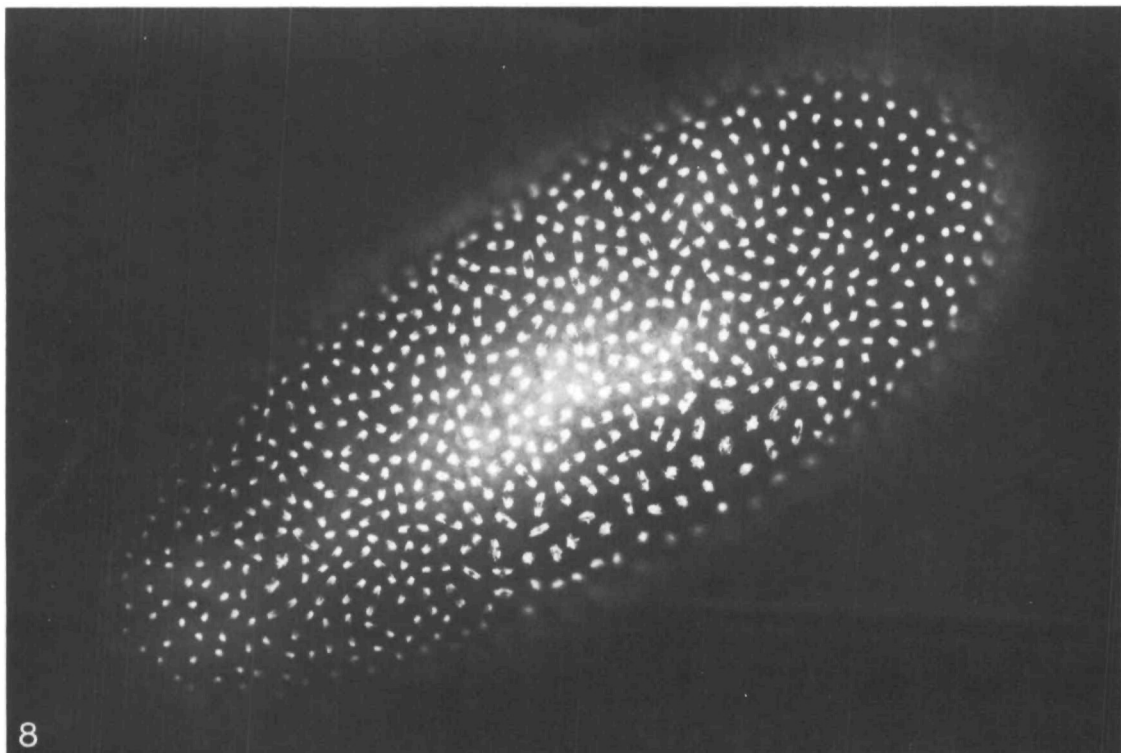


Fig. 8. A mitotic wave visualized in a embryo that was fixed and stained with Hoechst dye 33258 during the mitosis that concludes cycle 12. The nuclei at the poles are more advanced than are the equatorial nuclei; the equatorial nuclei here are still in anaphase (un-separated daughter sets of chromosomes visible), while the more poleward nuclei are entering telophase (chromosome sets separated and nuclear membranes reformed). $\times 360$.

the fixative to traverse the embryo from a single site of puncture). A later study of permeabilized embryos (Zalokar & Erk, 1976) interpreted as abnormal the occasional embryos displaying mitotic waves, since the majority of embryos visualized had their nuclei all in one phase. This distribution of phases, which we also find in our quick-frozen embryos (Table 3), is expected from the high speed of the waves seen in the live embryos. For example, chromosomes sit in their morphologically similar prometaphase-metaphase configurations for 1.9–2.8 min (see Tables 2 and 3), long

Fig. 7. A mitotic wave visualized in a living embryo during the mitosis that separates interphases 13 and 14. The number on each micrograph indicates the chronological developmental age of the embryo, which was determined as for Fig. 3. In each micrograph, the mid-embryo region that lies between the two arrowheads shows no distinct nuclear contours, indicating that the nuclei there are in mitosis. On the poleward side of each of these arrowheads, the small newly formed interphase nuclei of cycle 14 are visible. The mitotic wave at the anterior pole has started slightly before that at the posterior; the two waves converge towards the equator, as shown. For the embryo illustrated, the mitotic wave moved from each pole to the embryo equator in 2.5 min, a rate considerably slower than average (see text and Table 3). $\times 210$.

Table 3. *The metaphase to telophase transition observed in quick-frozen embryos: the detection of mitotic waves*

	Phase of embryonic nuclei during mitosis				
	Prometaphase	Metaphase	Both metaphase and anaphase	Anaphase	Both anaphase and telophase
Number of fixed embryos observed	31	21	14	14	8
Estimated duration (min) based on total metaphase-telophase interval of 2.5 min	1.1	0.8	0.5	0.5	0.5
Percentage of embryos revealing pole to equator mitotic waves*	(nd)	(nd)	100	28	100
Percentage of embryos having distribution of nuclei indicative of another pattern of mitosis†	(nd)	(nd)	None†	None	None

In order to capture the nuclear morphology of developing embryos without perturbation, the embryos observed here were quick-frozen at -70°C and fixed directly without dechorionization using a modification of the procedure of Mitchison & Sedat (see Materials and Methods). These embryos were stained with Hoechst 33258 and scored as described for Table 2. Data on the mitotic phases of cycle 10, 11 and 12 embryos (all of which display an identical period of about 3 min without a distinct nuclear envelope in live embryos, see Table 1) were collected and pooled. The transition from prometaphase to metaphase, which involves the disappearance of the nuclear outline (see legend to Table 2), is gradual and no attempt was made to detect waves across the embryo during this transition. Other possible transitions in nuclear phases were likewise difficult to score unambiguously, and are therefore not determined in this study (denoted 'nd' in Table).

* In about half of these embryos, a gradient of mitotic stages was observed in only either the anterior or posterior half of the embryo, and/or there was an abrupt transition in cycle phase at the equator. This is expected from the observations on living embryos that reveal that mitosis often starts on one pole before the other. The 28% of the embryos with all nuclei in anaphase and the 38% of those with all nuclei in telophase displayed conspicuous pole to equator gradients from late to early anaphase and late to early telophase, respectively.

† In this sample of 101 embryos, we observed no embryos with a gradient of mitotic phases that had other than a pole to equator orientation. However, we have occasionally observed mitotic gradients with different orientations in other batches of fixed embryos.

enough for many quick-frozen embryos to be found that have all their nuclei with chromosomes in a similar metaphase-like configuration (see legend to Table 2). We therefore conclude that mitotic waves reflect the normal, rather than the abnormal situation in *Drosophila*. Mitotic waves have also been documented in a considerable number of other syncytial insect embryos (reviewed by van der Meer, Kemmner & Miyamoto, 1982).

Mitotic waves are associated with cytoplasmic movements

Time-lapse cinematography of the syncytial embryos reveals that the above mitotic waves are associated with major movements of the inner yolk mass and of the peripheral cytoplasm (periplasm). At the end of interphase in each nuclear cycle, both ends of the yolk mass at the core of the embryo suddenly move inward, away from the poles. Simultaneously, the periplasm surrounding this yolk mass begins to flow towards the two poles. This movement begins in the region of cytoplasm nearest to each pole, and continues as cytoplasm nearer to the equator is recruited into one of the two opposing streams. The visual impression is that of a change in the consistency of the periplasm just behind the wave front. After the peripheral cytoplasm of the entire embryo has thus moved, the yolk slowly moves outwards and the entire sequence is repeated in reverse, again starting at the poles but with the cytoplasmic flow in the opposite direction. At the end of these events, the visible particles moved by the stream (including nuclei and somatic buds) appear to have been returned to their original positions. The magnitude of these flows varies considerably between embryos and between cycles in a single embryo, but they can move cytoplasmic particles, somatic buds and nuclei back and forth by as much as 100 μm during some mitoses. Our observations on *D. melanogaster* agree in all major features with those made on *Drosophila montana* by Kinsey (1967) and Wilson (1970).

The above sequence of yolk movements and periplasmic flows, coordinated with the nuclear-cycle phases, is illustrated diagrammatically in Fig. 9. While it is difficult to determine exactly the phase of mitosis in living embryos, it appears that the front of the poleward periplasmic flow is associated with the metaphase-anaphase transition, while the front of the reverse flow is correlated with the late telophase-early interphase transition. The first conclusion is based on the observation that in cycle 13 the nuclear contours disappear before the onset of the poleward periplasmic flow, while the second is based on the reappearance of discrete small nuclei at the front where reverse flow begins.

An analysis of the magnitude and duration of the yolk movements at the anterior pole of two embryos is presented in Fig. 10 and described in the legend. In the embryos observed, the yolk contractions at opposite ends of the embryo, like the mitotic waves with which the contractions are coordinated, began within 2 min of each other, and they frequently began simultaneously. Injection of cytochalasin E into the syncytial embryo, to an internal concentration of about 200 $\mu\text{g}/\text{ml}$, halts both the yolk movements and the associated periplasmic flows, while appearing not to interfere with the nuclear divisions (Table 4). This result rules out the possibility that the yolk contractions are the cause of the nuclear-phase changes.

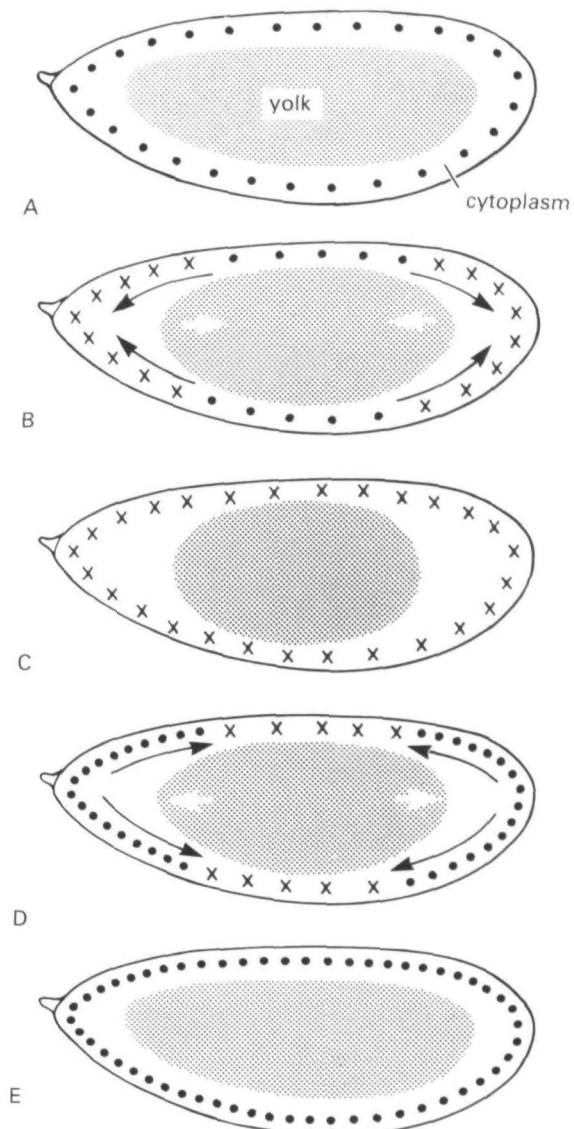


Fig. 9

The magnitudes of the yolk contractions in *D. melanogaster* are rather constant between embryos (see Fig. 10). In contrast, the magnitude of the periplasmic flow varies considerably; because of this and the results of the cytochalasin injections, it seems likely that the periplasmic flow is only a secondary phenomenon, resulting from internal pressures caused by the yolk contraction.

In our preliminary study, injection of colchicine into cycle 10–12 embryos, to a final concentration of 40 µg/ml, stopped both the yolk movements and the periplasmic flow, as well as the nuclear division cycle (Table 4). Thus, the nuclear cycle may induce the yolk contractions; alternatively, these could be separate events that both require microtubule function (but see legend to Table 4).

The core of the embryo contains long fibres and polyploid nuclei

After the majority of the nuclei migrate outwards to reach the embryo periphery in cycle 9, a smaller number of nuclei, termed yolk nuclei, remain behind in the interior, still surrounded by the yolk particles that fill the core of the embryo (Fig. 1). Observations of mitotic figures in fixed and stained embryos reveal that the yolk nuclei undergo mitosis in approximate synchrony with the migrating somatic nuclei during cycles 8 and 9, and divide a little later than the somatic nuclei in cycle 10; thus the yolk nuclei are in telophase of cycle 10, when the majority of the nuclei have already entered interphase 11. After this time, no further synchronous division of the yolk nuclei is seen. Because the visibility into the core of the embryo is obscured, scattered

Fig. 9. A schematic representation of yolk and cytoplasmic movements. These diagrams are based on observations of nuclear cycles 11 and 12; mitosis 13 follows a somewhat different pattern (see Fig. 10). The central mass of yolk-containing cytoplasm is stippled, while the yolk-free peripheral cytoplasm is untextured. (●) Nuclei in interphase, prophase, or metaphase; (X) nuclei in anaphase or telophase. Only the peripherally located nuclei in one optical section are depicted; pole cells are not shown. The relative size of the yolk mass is reduced and the scale of the yolk movements is exaggerated for clarity.

- A. The embryonic nuclei are all in interphase.
- B. Just after the nuclei pass from interphase into mitosis, the yolk mass retracts from both poles. Simultaneously, the peripheral cytoplasm (periplasm) begins to flow from the equator towards the polar regions. The periplasm nearest to the poles moves first, followed by a progressive recruitment into the stream of poleward flow of more and more equatorial material. The zone where periplasm is being recruited into the stream, which progressively shifts from each pole to the equator, seems to coincide with the region where nuclei enter anaphase (see text). Note that the direction of periplasmic flow here is counter to both the direction of the shifting front of cytoplasmic recruitment and the direction of the mitotic wave.
- C. The nuclei are all in a late phase of mitosis (anaphase or telophase).
- D. The yolk mass relaxes and re-enters the regions near the poles. The initiation of this yolk movement appears to touch off a chain of periplasmic movement as in B, except that this time the periplasm flows from each pole back towards the equator. The front of the periplasmic movement coincides with passage of the nuclei into their next interphase and with the start of the budding cycle. Note that the direction of periplasmic flow, the front of periplasmic recruitment, and the mitotic wave are all travelling in the same direction. While the initial yolk retraction in B is rapid, the yolk relaxation here is slow and persists for much of interphase (see Fig. 10).
- E. Mitosis is over, and all of the nuclei are in their next interphase.

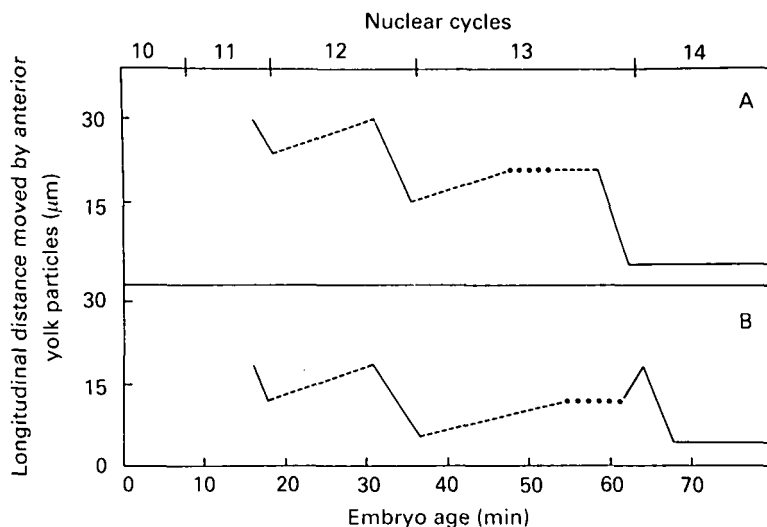


Fig. 10. The developmentally timed movements of the central yolk mass, compared in two different embryos at 22–25 °C. Age is designated both in minutes from the start of cycle 10 (as in Fig. 3), and by nuclear-cycle phase. The yolk moves as a coherent mass, with the yolk particles generally retaining their spatial relationships to their neighbours. The ordinate denotes the absolute distance along the long axis of the embryo (in μm) of individual yolk particles followed at the anterior tip of the central yolk mass; this is plotted *versus* the developmental age of an embryo. Measurements were made from time-lapse video tapes, and distances measured relative to a fixed point on the video screen. Because the embryo plasma membrane undergoes little if any coherent longitudinal movement at this time, the yolk movements cause a corresponding change in the distance between the tip of the yolk mass and the anterior tip of the embryo. (—) Rapid retractions of the yolk away from the pole; (---) slower yolk 'relaxations' towards the pole. As described for Fig. 9, each of the sudden yolk retractions appears to begin when the nearby anterior pole nuclei enter anaphase. Note that an unusually large inward movement of the yolk mass occurs at the mitosis that ends cycle 12, which may be related to the fact that a large increase in the depth of the periplasm is occurring at this time.

In all embryos thus far studied, a 3–6 min period of dramatic calm occurs late in cycle 13 (· · ·), during which both the yolk movements and the saltatory movement of particles in the periplasm cease completely. In embryo A, the calm was followed by a rapid contraction that signalled the end of cycle 13, while in embryo B, a sudden poleward movement of the yolk preceded this sharp contraction. The latter seems to be the more common pattern. Note that the yolk remains contracted during all of interphase 14, in contrast to the gradual yolk relaxation that occurs during the interphases of previous cycles. Later, extensive yolk movements accompany gastrulation (not shown).

mitoses of single yolk nuclei would probably escape detection. We have therefore compared the number of yolk nuclei in fixed whole embryos at cycles 11 and 14. As shown in Table 5, the number of yolk nuclei stops increasing after cycle 10, remaining constant at about 200 during cycles 11 through 14, consistent with our failure to observe mitotic figures. However, the intensity of yolk nuclei fluorescence increases progressively, reflecting their increasing polyploidization. The morphology of the yolk nuclei during nuclear cycle 14 is illustrated in Fig. 11B, C, for comparison with the cycle 9 yolk nuclei displayed in Fig. 11A. The distinctive behaviour of the yolk nuclei suggests that they may play an important role in *Drosophila* embryogenesis.

Table 4. Effect of the microinjection of inhibitors on cytoplasmic movement

Inhibitor	Intracellular concentration ($\mu\text{g}/\text{ml}$)	Stage of embryo injected	Effect
Colchicine	1.5	14	Saltation persists ($N = 2$)
	8	14	Saltation blocked ($N = 2$)
	40	14	Saltation blocked ($N = 9$)
	200	14	Saltation blocked ($N = 1$)
Cytochalasin E	200	14	Saltation persists ($N = 5$)
Colchicine	40	10–12	Yolk contractions blocked ($N = 2$)
Cytochalasin E	2	10–12	Yolk contractions normal ($N = 2$)
	20	10–12	Yolk contractions abnormal ($N = 3$)
	200	10–12	Yolk contractions blocked ($N = 2$)

The effect of each inhibitor on the living embryo was monitored using time-lapse cinematography (see Materials and Methods). Some of the cycle 14 embryos were injected with 40 $\mu\text{g}/\text{ml}$ colchicine during the first 10 min of cycle 14, while others were identically injected 20–40 min into this cycle. In the embryos injected early, the nuclei never elongated, and no cleavage furrows appeared between the nuclei (see Fig. 5 for the cellularization sequence in a normal embryo). In the embryos injected later, when nuclear elongation had already occurred, the incipient cleavage furrows continued to grow between the nuclei forming apparently normal cells, and early gastrulation movements began on schedule. Cinematography was started 5 min after each injection and the effects of the inhibitors were complete by this time. The only exception involved the different manner in which the yolk contractions responded to the two inhibitors tested: whereas the colchicine injection (40 $\mu\text{g}/\text{ml}$) stopped yolk contractions immediately, cytochalasin (200 $\mu\text{g}/\text{ml}$) allowed one cycle of yolk contraction before blocking further movement. In similar studies on the gall midge *Wachliella*, a lower concentration of colchicine was found to depolymerize most microtubules without blocking the yolk contractions (Wolf, 1978).

Table 5. The yolk nuclei cease dividing after mitosis of cycle 10

Developmental stage	Total number of yolk nuclei per embryo
11	226
	200–216
	190–216
14	227
	204–212
	185
	179
	147–163

Nuclear counts were made from stacked transparent photographic enlargements of serial optical sections of individual fixed and stained embryos. An example of one such embryo is shown, in a single plane of focus, in Fig. 11c. Each row in the table presents the data for a single embryo. A range of values is given in those embryos where a cluster of closely neighboring nuclei made it impossible to be certain of their exact number.

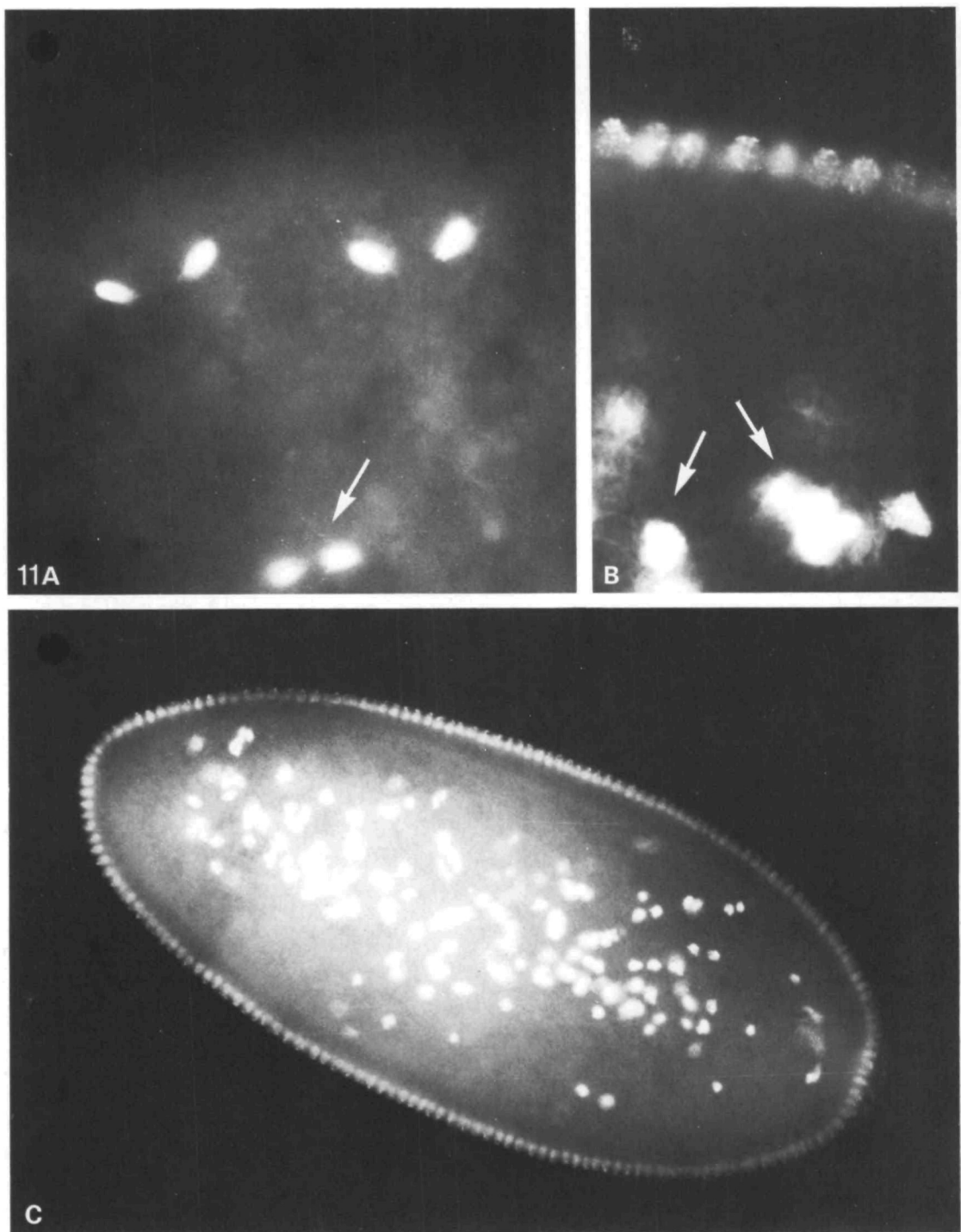


Fig. 11

Spectacular arrays of very long fibres of apparently uniform diameter are also present in the core of the embryo, as seen in our preparations of squashed embryos (Fig. 12). The fibres are stiff but flexible, and those that are doubled back on themselves bend in broad smooth curves (see Fig. 12A). Single fibres are very long, unbranched, and in fresh preparations free ends are infrequently seen (lengths of greater than 500 μm are common). These fibres are numerous, are found throughout the nuclear cycle and occur in embryos of all stages studied (newly laid eggs through cycle 14 embryos were examined). Large numbers of free fibres are present in squash preparations of the cellularized stage 14B embryos, in which most cells remain intact. We therefore conclude that these very long fibres are abundant in the central yolk mass.

The long fibres persist in a solution containing 0.02 M-Ca²⁺ (data not shown), are stable at high salt concentration (up to 10 times concentrated buffer AM was tested), but breakdown rapidly under low salt conditions (2 mM-phosphate buffer, pH 7.2; R. Marcos & V. E. Foe, unpublished observations). These fibres also fall apart in physiological salt to which 0.05% Triton X-100 has been added, conditions under which actin filaments, microtubules and intermediate filaments are all stable (Schliwa, van Blerkom & Porter, 1981; Heuser & Kirschner, 1980). However, these fibres are too thick to be a simple filament of any type. Moreover, whenever they become adsorbed to a microscope slide, a thick halo of material quickly spreads out from each fibre, as illustrated in Fig. 12B. It therefore seems that whatever their underlying filament type, these fibres are coated with a substantial layer of bound cytoplasm. We suggest that Triton X-100 removes this layer of adherent cytoplasm, and thereby destabilizes the filament.

A rapid relocation of presynthesized materials appears to be mediated by cytoskeletal elements

Observation with DIC optics reveals that the peripheral cytoplasm of live syncytial blastoderm embryos has a somewhat fibrous appearance, with the fibres oriented perpendicular to the embryonic surface (Fig. 4). Observation of living embryos at high magnification reveals an extensive saltatory movement of particles in the direction of these fibres: particles with a diameter of about 0.5 μm move outward from the yolk to the plasma membrane and back, with no detectable movement in a direction parallel to the surface. The orientation of this saltatory movement is represented

Fig. 11. Fixed, Hoechst 33258-stained embryos chosen to illustrate nuclear migration during cycle 9 and the increase in ploidy of the yolk nuclei between cycles 9 and 14.

A. Detail of an optical mid-section of a cycle 9 embryo showing three pairs of nuclei in telophase. The two pairs of outward-migrating nuclei, which were fixed just as they were beginning the final phase of their migration to the surface (see Fig. 2), stain with equal brightness to the non-migrating pair of yolk nuclei (arrow). $\times 1300$.

B. Detail of an optical mid-section of a cycle 14 embryo comparing the peripherally located somatic nuclei with the much more brightly staining yolk nuclei (arrows), which have become polyploid. $\times 1300$.

C. Optical mid-section of a cycle 14 embryo showing the peripherally located somatic nuclei and the internally located yolk nuclei. $\times 348$.

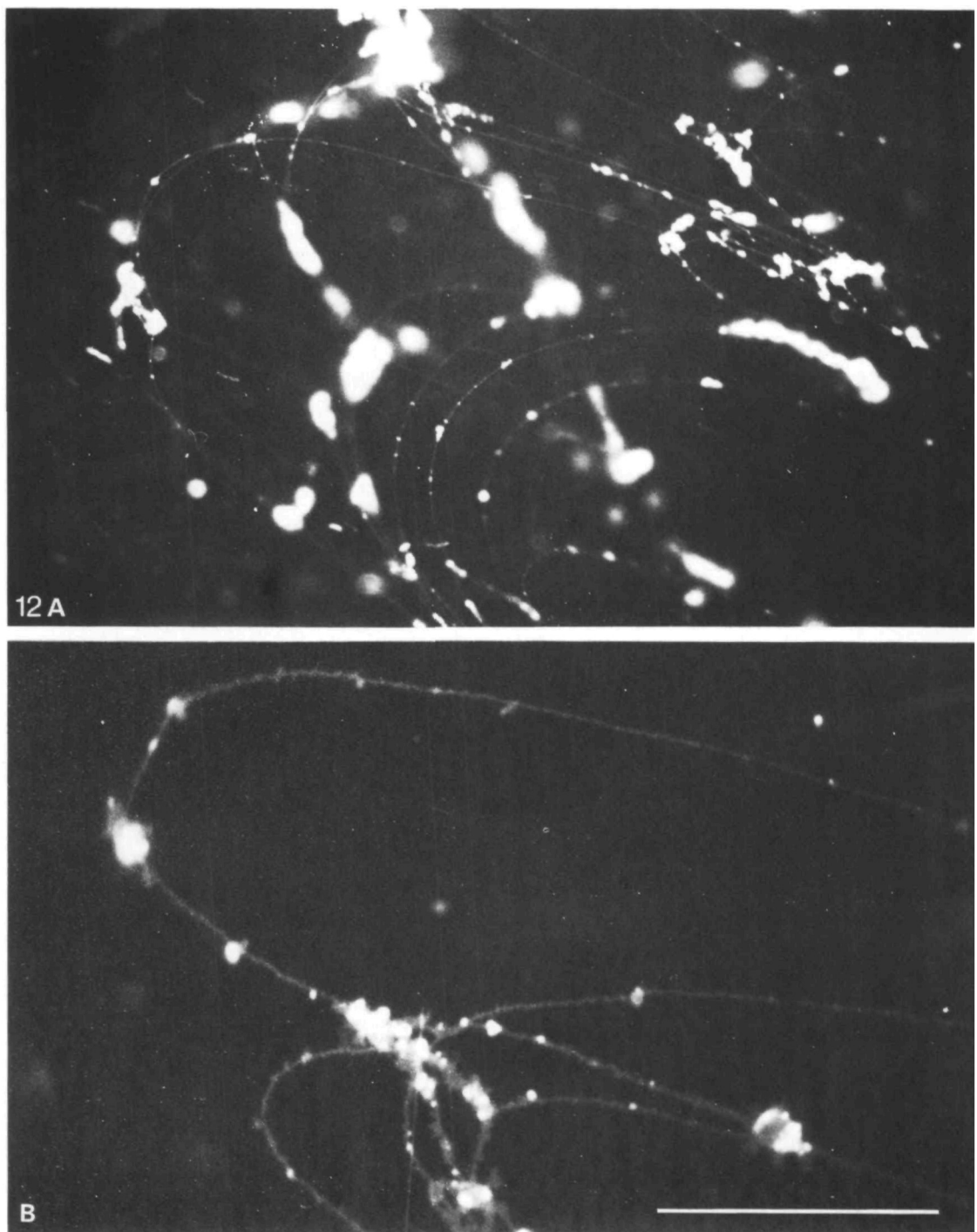


Fig. 12

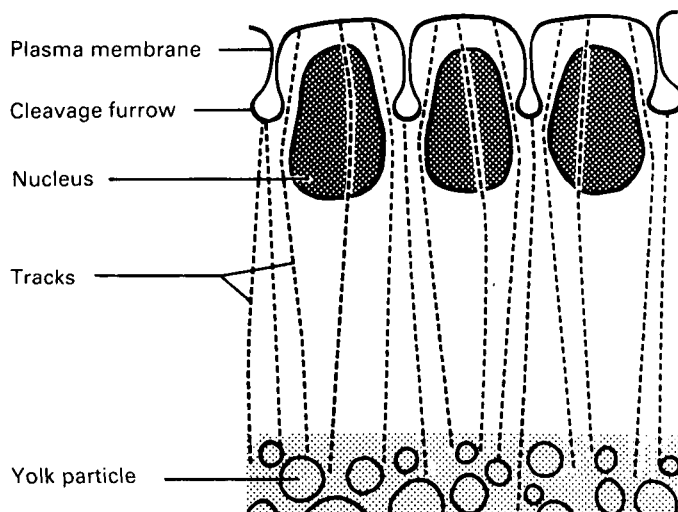


Fig. 13. Schematic illustration of oriented particle movement between the central yolk mass and the egg membrane in living embryos. This drawing was derived from tracings of a time-lapse video tape made of a living embryo. All tracks identified by virtue of the movement along them of visible particles are indicated (----); the depth of focus was probably less than $1.0 \mu\text{m}$. At the stage illustrated here (early cycle 14), cleavage furrows were forming between the peripheral nuclei. The microtubules thought to mediate this transport (see below) may extend as far as the yolk nuclei, close to which clusters of centrioles are found (Rickoll, 1977). Because visibility into the central yolk mass is poor, it is not known how far these tracks extend into the core of the embryo.

diagrammatically in Fig. 13. Analysis of these moving particles using videotapes demonstrates a polarized movement with a traversal speed of about $1.7 \mu\text{m}/\text{s}$ in the outward direction and a return speed of about $0.6 \mu\text{m}/\text{s}$. Outward travelling particles were observed to move continuously over distances of at least $4.5 \mu\text{m}$. Return movements were characterized by a more intermittent type of motion.

The saltatory movement of particles can first be detected just as the nuclei reach the surface during cycle 10, and increases progressively during the interphases of cycles 10–13, slowing slightly during mitoses 10–12. But during mitosis of cycle 13 there is a dramatic 3–6 min hiatus both in the saltatory movement and in the ongoing yolk movement (see legend to Fig. 10). Saltation then restarts abruptly at a high level, which is maintained through cycle 14. In favourable preparations of late stage 14A embryos, when the thickness of the periplasm is greatest, saltation can be observed in the peripheral cytoplasm to a depth of at least $40 \mu\text{m}$. Similarly oriented saltatory

Fig. 12. The long fibres released from a squashed-embryo preparation. Each micrograph displays only a small fraction of the total number of fibres released upon squashing a single cycle 9 embryo into buffer AM containing $2 \mu\text{g}/\text{ml}$ RITCB, which makes the fibres clearly visible by fluorescence microscopy (see Materials and Methods). A. A group of fibres floating free above the surface of the glass slide. These fibres appear to have a uniform diameter. B. Some fibres that have adhered to the glass surface of the slide, viewed at the same magnification as in A. Note the characteristic spreading out of material that leaves the fibre and attaches to the glass (see text). Bar, $100 \mu\text{m}$.

movements continue during stage 14B, even in the moving cells of the early gastrula. Radially directed, 'dancing' or 'jiggling' movements of large particles in the periplasm have been noted by others (Fullilove & Jacobson, 1971; Wilson, 1970), but were not further analysed.

Injection of colchicine into cycle 14 embryos, to a final concentration as low as $8 \mu\text{g}/\text{ml}$, rapidly halts the radially directed saltatory movements (see Table 4, above). In early cycle 14 embryos (nuclei not yet elongated, see 64 min panel in Fig. 5), this injection prevented cell membranes from developing between the nuclei and the nuclei themselves remained rounded, became swollen, and eventually moved relative to each other to form irregular, multiple layers in the periplasm (see also Zalokar & Erk, 1976). However, when colchicine was injected into slightly older cycle 14 embryos (nuclei already elongated, see 75 and 93 min panels in Fig. 5), cell membrane growth continued to completion, and gastrulation movements began that were normal in appearance even though there were no saltatory movements. A very different result

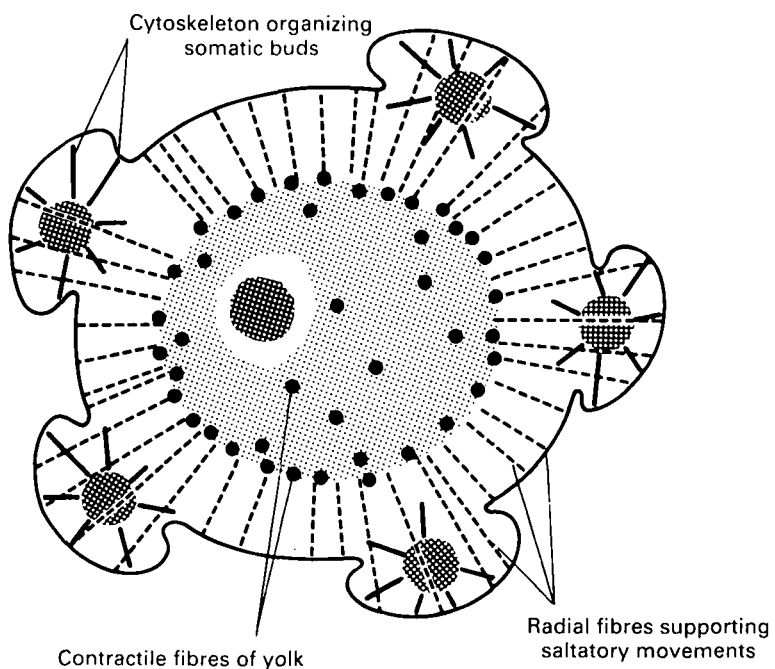


Fig. 14. Schematic drawing of a syncytial blastoderm embryo in cross-section, depicting the three levels of cytoskeletal organization inferred from this study. (1) The cytoplasm and plasma membrane around each nucleus are organized, creating a somatic bud. (2) Radial tracks, presumably fibres, in the peripheral cytoplasm orient saltatory movements in a direction perpendicular to the embryo surface. The radial fibres begin at the plasma membrane and disappear from view as they enter the interior yolk region of the embryo. (3) Contractile fibres are proposed to organize the longitudinal contractions of the yolk mass. The orientation of these fibres is inferred from the directions of movement of the yolk mass. We have arbitrarily located longitudinal contractile fibres both in the central yolk mass and ensheathing it. Five peripherally located nuclei and one yolk nucleus are depicted in this diagram.

was obtained with cytochalasin; its injection into either early or late cycle 14 embryos (to a final concentration of 200 µg/ml) caused any partially formed cell membranes present to disappear, without abolishing the radially directed saltatory movement of particles.

Electron microscopic studies have revealed microtubules with the approximately radial orientation of the saltatory tracks (Fullilove & Jacobson, 1971; Rickoll, 1977). Because of the sensitivity of saltation to colchicine, these microtubules are likely to be required for the movements observed. In addition, a poorly defined network of filamentous structures can be seen at the base of the cleavage furrows in fixed cycle 14 embryos (Mahowald, 1963; Rickoll, 1976). The dramatic effect of cytochalasin on the forming cleavage furrows would be explained if these were actin filaments essential for maintenance of the inward extension of the growing plasma membrane.

Fig. 14 summarizes in a schematic way our current view of the three domains of cytoplasmic organization in the *Drosophila* embryo that have been discussed: the structured cytoplasm around each nucleus, the longitudinal order that gives coherence to the contractile core of the embryo, and the radially directed fibres that mediate saltatory transport through the periplasm. It is not known what relation the long fibres displayed in Fig. 12 bear to these cytoplasmic domains, nor how many different types of cytoskeletal elements are involved in each region.

DISCUSSION

This study of the syncytial blastoderm stages of *Drosophila* embryogenesis was undertaken in order to increase our knowledge of the cytological events that accompany the important cell determination processes that take place at this time. It seems likely that the elaborate cytoplasmic organization that we have detected in these embryos plays a role in providing the positional information that is used to determine the fate of the nuclei in the pre-cellular embryo. In the discussion that follows, we review the possible relevance of our observations to the mechanisms involved in *Drosophila* development.

Positional information is specified in a single cell

Mutations exist in *Drosophila* that affect the organization of the developing embryo in a global way, altering the dorsal–ventral or the anterior–posterior polarity. Both maternal (Bull, 1966; Nusslein-Volhard, 1979; Nusslein-Volhard, Lohs-Schardin, Sander & Cremer, 1980) and zygotic (Nusslein-Volhard, personal communication) mutations of this type are known. These mutations demonstrate that the determination of the embryo polarity depends partially on the initial organization of the egg, but also partially on the activity of the embryonic nuclei. The effects of the mutations can be detected at the first moments of gastrulation by the abnormal patterns of invagination of the blastodermal cell sheet. The fact that gastrulation begins in cycle 14, before separation of the forming blastoderm cells from the yolk is complete (Rickoll, 1976; Rickoll & Counce, 1980), leads us to conclude that important spatial patterns must be set up in the embryo while it is still in a syncytial state.

The earliest visible sign that the somatic nuclei in cycle 14 embryos are not identical is the spatially patterned differences in their cycle lengths, as reported in Fig. 6. This difference between cells is consistent with assays that reveal that the cells that form in cycle 14 have become committed to specific developmental fates according to their position in the embryo. Thus, when anterior blastoderm cells are dissociated and cultured *in vivo* (Chan & Gehring, 1971) or when single anterior blastoderm cells are ectopically transplanted (Illmensee, 1978), they retain their ability to make adult head and thoracic structures. It seems that at this stage the ectodermal cells of the blastoderm are restricted in their developmental fate to contribute to the epidermis of only a single segment, but that the precursor cells to many of the specific structures within a segment (such as the wing or leg imaginal discs) have not yet been specified (for a review, see Lawrence, 1981). At 'cellular blastoderm' (see Fig. 1), the cells that will give rise to each segment are thought to consist of a partial ring, three to four cells wide, with the rings that represent successive segments serially aligned along the anterior-posterior axis of the embryo (Lohs-Schardin, Cremer & Nusslein-Volhard, 1979).

In other experiments, preblastoderm embryos have been 'ligated' into separate anterior and posterior fragments to assess the developmental potential of these fragments at different times during development. Newman & Schubiger (1980) found that embryos ligated into anterior and posterior halves just prior to nuclear migration, that is during nuclear cycles 6 through 9, develop into embryos in which all of the nuclei in the posterior fragment participate in formation of only a few of the most posterior segments. The segments formed, which are much larger than normal, contain many more cells per segment than in the normal embryo; thus, for example, nuclei that would normally have given rise to cells of the 4th abdominal segment in an unligated embryo became determined to form 6th abdominal segment structures instead. When the same ligation was performed during cycles 10, 11, and 12, the posterior fragments contained more of the abdominal segments, though the first few (most thorax-proximal) abdominal segments were still missing. Ligations performed at the cellular blastoderm stage or shortly thereafter usually produced a complete, normal set of segments (Schubiger & Wood, 1977; Vogel, 1977). In addition to suggesting that the system that assigns nuclei to specific segments is being patterned in a gradual manner throughout the syncytial blastoderm stages, the ligation experiments reveal that normal cell determination processes require interactions along the anterior-posterior axis of the embryo (Schubiger *et al.* 1977).

The normal developmental process produces the same number of segments in eggs of a range of sizes. For example, some abnormally small eggs (about two-thirds normal size) occur spontaneously in our populations, and a substantial fraction of these eggs can be shown to develop into embryos that have a normal number of segments, with each being smaller than normal (unpublished observations of V. E. Foe). This observation, when combined with the experiments of Newman & Schubiger (1980) described above, seems to indicate that the mechanism that specifies these segments neither counts nuclei nor measures absolute distances along the embryo.

In summary, the fate of nuclei appears to be determined according to their *relative* positions along the anterior-posterior axis of the *Drosophila* embryo. This regulative property is common to many developmental fields (Wolpert, 1969). Segment formation in *Drosophila* may therefore provide a relatively accessible general model for studying the fundamental processes by which cells acquire positional information in developing systems. A striking feature of the *Drosophila* system is that this information is set up in a syncytial single cell. If the mechanism used in *Drosophila* is a general one, the basis for imparting positional information must be independent of the isolation of one cell from another by cell membranes that occurs in most embryonic fields. An analogous conclusion has been reached from studies of pattern formation in ciliates (reviewed by Aufderheide, Frankel & Williams, 1980).

Each nucleus is associated with a domain of structured cytoplasm

As shown both in this report, and in the electron micrographs of Turner & Mahowald (1976), each peripheral nucleus in the syncytium organizes an extensive region of cytoplasm and plasma membrane around itself to form a 'somatic bud'. Furthermore, each premigrational nucleus exists in an 'island' of relatively yolk-free cytoplasm and, when it migrates to the periphery, it does so in this island (Rabinowitz, 1941a,b). Once at the periphery, the domain of cytoplasm associated with each nucleus in a somatic bud seems to divide every time that the nucleus divides, and there is a continuous decrease in the size of the somatic buds as one progresses through the syncytial blastoderm stages (see fig. 11 of Turner & Mahowald, 1976). This raises the possibility that a structured cytoplasmic domain that organizes the bud is conserved and partitioned to the daughter nuclei each time that a nucleus divides.

It seems logical to suggest that the structured cytoplasm around each nucleus involves cytoskeletal elements. These could be organized by the region containing the centriole pair that, at least during interphase of cycle 14 (and probably during earlier cycles), is located between the nuclear envelope and the embryo surface (Rickoll, 1977; see also Huettner, 1933). The fact that, as each peripheral nucleus swells during interphase, its associated cytoplasm creates an outbudding of the embryonic surface (the somatic bud, see Fig. 4; Foe, unpublished) suggests that some of these elements attach to the plasma membrane. Indeed, evidence for a dynamic association between plasma membrane and nuclei involving the centriole has come from studies of the nuclear migration stages of the embryo of another dipteran: in the gall midge, *Wachtliella persicariae*, saltatory movements of yolk particles observed in living embryos reveal the existence of a cytaster associated with each nucleus, whose microtubules extend from the centriole in the centre of the cytaster to the embryo periphery on one side, and from this centre to the nucleus on its opposite side (Wolf, 1978). In *Drosophila*, electron micrographs of embryo exteriors reveal numerous microprojections on the plasma membrane of each bud, but not between adjacent buds (Fullilove & Jacobson, 1971; Turner & Mahowald, 1976, 1977; Swanson & Poodry, 1980). These microprojections could mark membrane attachment points for cytoskeletal elements.

The perinuclear cytoplasm may allow nuclear determination without a plasma membrane

In recent experiments, a monoclonal antibody has been used to detect a protein antigen that appears to be confined to the local domain of cytoplasm surrounding each nucleus in cycle 10–12 *Drosophila* embryos, being absent from the cytoplasm between adjacent somatic buds (H. Saumweber & J. Sedat, personal communication, 1982). This observation demonstrates that proteins do not mix freely in the syncytial cytoplasm, and raises the possibility that different proteins could become confined to the cytoplasmic domains that surround different nuclei.

Some results of nuclear transplantation experiments are readily interpreted in this context. It has been shown that the embryonic nuclei, before migration to the periphery (cycle 6–9), are totipotent when injected together with their enveloping cytoplasm back into host embryos of similar age (Okada *et al.* 1974). It has also been shown that early gastrula-stage *nuclei* can support development when injected singly, and with a minimum of adhering cytoplasm, into unfertilized eggs (Illmensee, 1973). On the basis of these latter experiments, it was concluded that cycle 14 nuclei have a less restricted developmental potential than do the determined cells in which they reside (Chan & Gehring, 1971; Illmensee, 1973, 1978). Hence it was concluded that a cell is the smallest autonomous unit of determination and that transplanted nuclei are more readily reprogrammed than are transplanted cells. This conclusion made it appear impossible to carry out a direct test of the developmental commitment of the non-cellularized nuclei from the syncytial blastoderm stages. However, Kauffman (1980) has recently reported transplantation experiments that demonstrate that some of the cycle 13 syncytial nuclei, if transplanted with adhering cytoplasm, have already acquired either an anterior or a posterior commitment that survives their transfer to an ectopic site in another embryo of the same age. To date, it has not been possible to demonstrate a segmental commitment in these nuclei (Kauffman, 1981). However, these experiments indicate that nuclei transplanted with adhering cytoplasm can carry a stable pattern of determination with them, despite the expected rapid mixing of soluble components between donor and host nuclei caused by normal diffusion processes. We suggest that this commitment is caused by determinants that become tightly associated with the perinuclear domains of cytoplasm during the syncytial blastoderm stages. In this view, the observed low frequency of reprogramming of host nuclei by the cycle 13 transplants (Kauffman, 1980) could reflect an occasional transfer to a nearby host nucleus of cytoplasmic components associated with a donor nucleus.

Blastodermal mitotic waves are unlikely to have an important organizing role in pattern formation

From where might the determinants that provide positional information to the blastoderm nuclei originate? It has been suggested by others that patterned mitotic waves could generate region-specific differences in interphase lengths of the blastoderm

nuclei, which in turn could produce local differences in transcription or heterochromatinization patterns (Agrell, 1964; Kauffman, 1975); such differences could thereby provide information to the nuclei with regard to their relative locations along the embryo. However, the mitotic waves that we observe in the syncytial embryo do not tend to create significant or reproducible differences in interphase length. Evidence against the more general proposal comes from the recent experiments of van der Meer *et al.* (1982), Miyamoto & van der Meer (1982) and Wolf (1983), which indicate that the normal direction of the mitotic waves can be reversed in insect eggs of other species without preventing the production of normal embryos.

There is a long-range organization throughout the embryonic cytoplasm

As we have described (Fig. 9), the mitotic cycle is coordinated with a major yolk contraction seen once in each cycle, which begins during the metaphase to anaphase transition in the nuclei at each pole. Injection of colchicine into syncytial *Drosophila* embryos stops both nuclear division and yolk contractions, whereas injection of high concentrations of cytochalasin stops only the yolk contractions (Table 4). Thus, the nuclear transition could induce the yolk contraction directly, or these could be separate events, both of which are induced by a third invisible wave (such as a local change in free Ca^{2+} concentration) that originates near each pole once in each nuclear cycle.

Although the yolk contractions themselves are unlikely to be central to cell determination processes, they reveal the existence of an organized coherent yolk mass. Whatever their nature, the contractile elements of the yolk must be capable of supporting not only the rapid yolk contractions seen near the end of nuclear cycles 9 through 13 and the sustained contraction of interphase 14, but also the rapid yolk *expansion* that frequently occurs between cycles 13 and 14 (Fig. 10). Because of the observed yolk movements, we have postulated that there are longitudinally oriented contractile filaments running through the central yolk mass and/or at its periphery (see Fig. 14). The sensitivity of the contractility of the yolk to cytochalasin suggests an involvement of actin filaments. In fixed, cycle 14 *Drosophila* embryos a system of actin filaments has been observed with thin-section electron microscopy at the periphery of the yolk mass (Rickoll & Counce, 1980). While we do not know the nature or *in vivo* orientation of the many long, cytoplasm-coated fibres seen in our squashed embryo preparations (Fig. 12), these are also likely to be important for the organization of the yolk-containing core of the embryo. Further detailed studies of these interesting long fibres are clearly warranted.

Once the nuclei appear at the periphery, fibrous elements can be seen to radiate outwards from the yolk towards the egg plasma membrane (Figs 4, 13). These fibres are likely to mediate the rapid saltatory movement of particles between the yolk and the exterior of the embryo. Both microtubules and actin filaments have been postulated to be involved in saltatory movements (Rebhun, 1972). The fact that the observed saltatory transport is sensitive to colchicine, but not to cytochalasin, implicates microtubules in this process in *Drosophila* (Table 4).

The large particles whose saltatory transport we have visualized have the proper

size and intracellular distribution to be mitochondria; however, it is very probable that many other, less visible materials are also carried by this radially directed transport system. There is an especially rapid mobilization of particles during cycles 13 and 14, which is correlated with the enlargement of the peripheral, yolk-free cytoplasm that occurs at this time. This widening of the peripheral cytoplasm is known to be blocked by colchicine (Zalokar & Erk, 1976); one might therefore expect the radially directed transport system to carry the materials necessary for the construction of the clear cytoplasm that will later be incorporated into the cells that form during cycle 14. One might also anticipate that this transport system would convey materials needed for the very rapid plasma membrane growth that characterizes cycle 14 embryos. However, it is noteworthy that in our experiments inhibition of saltatory movement by colchicine did not stop membrane growth once such membrane growth had begun in cycle 14 (see legend to Table 4).

There is a striking transient arrest of both saltatory motion and yolk movement that occurs between cycles 13 and 14 in normal embryos (Fig. 10). This calm immediately precedes the process of cellularization, which will occupy much of cycle 14, suggesting perhaps that it reflects a period of cytoskeletal reorganization. The period of calm is succeeded by an elongation of the nuclei that seems to require microtubules, and by the growth of the plasma membrane between these nuclei that seems to require actin filaments (Table 4; and Zalokar & Erk, 1976).

Could the cytoskeleton of the embryo be important in cell determination processes?

Most models ascribe the acquisition of positional information by the nuclei to their concentration-dependent response to gradients of diffusible morphogens (i.e., see Meinhardt, 1977; Kalthoff, 1979; Nusslein-Volhard, 1979; Sander, 1975; Schubiger & Wood, 1977). These models require that smooth concentration differences are maintained across short distances. The extensive cytoplasmic flows that we have observed in *Drosophila* embryos during each mitosis (see Results and Fig. 9) pose difficulties to the maintenance of gradients of morphogens if these morphogens are free in the cytoplasm. Indeed, combined egg centrifugation and ultraviolet irradiation experiments have suggested that the anterior determinants found in *Smittia* eggs do not occur as freely diffusible molecules (Kalthoff, Hanel & Zissler, 1977). How else might a gradient of positional information involved in segmental determination be established?

As discussed, our observations suggest that the yolk that fills the core of the early *Drosophila* embryo is traversed by an extensive array of cytoskeletal elements that run in a longitudinal direction between its anterior and posterior poles. This highly organized cytoskeletal core of the embryo forms a substrate on which a gradient of morphogenetic substances could be generated. Such a hypothetical gradient could help to carry positional information in the embryo, either alone, or, via its effect on the transcriptionally active polyplloid yolk nuclei that remain embedded in it in early development. In either case, differences in the concentrations of substances in the core of the embryo could be faithfully projected to the somatic nuclei at the egg surface, because of the organized transport system that radiates from this core (Fig. 13). This

difference in concentration might in turn inform each nucleus as to its relative location along the anterior-posterior axis of the embryo.

Circumstantial evidence for the involvement of some solid cytoplasmic matrix in establishing an anterior-posterior information gradient comes from experiments on a hemipteran, the pea beetle, *Callosobruchus*. Here, temporary constriction of syncytial embryos produces double abdomen larvae in which reversal is often restricted to longitudinal strips of the larval cuticle (van der Meer, 1983). Also relevant are centrifugation experiments with the eggs of the dipteran, *Smittia*, which have shown that the location of the yolk particles themselves is not important for laying down the pattern of the insect embryo (Kalthoff *et al.* 1977; for a review, see Kalthoff, 1979). Nevertheless, the cytoskeletal framework associated with these yolk particles could play a crucial role in development; indeed, since centrifuged eggs can reorganize themselves and develop normally, an organized cytoskeletal core is likely to persist in centrifuged *Smittia* embryos. It has not been possible to perform similar centrifugation experiments with *Drosophila* embryos, which are generally killed by large centrifugal forces.

An alternative initial source of the positional information required for segment determination in insect embryos is the egg plasma membrane, or a periplasmic layer that in centrifugation experiments remains closely associated with this membrane. With regard to the anterior-posterior decision in *Smittia*, combined egg centrifugation and irradiation experiments make these last two possibilities seem unlikely (Kalthoff *et al.* 1977). Cytoskeletal elements formed in response to the entering sperm seem to establish the dorsal-ventral axis in early *Xenopus* embryos (Gerhart *et al.* 1981). However, a critical test of the proposed central role of the cytoskeleton in generation of positional information in insect embryos has not been performed.

This work was supported by USPHS grant GM 23928 from the National Institute of General Medical Sciences of the National Institutes of Health and by a Senior Fellowship from the American Cancer Society to V.E.F. We wish to thank John Sedat and Tom Kornberg for their invaluable advice and for permitting us to make use of their laboratory facilities for part of this work. We thank John Sedat, Christine Nusslein-Volhard, Jitse van der Meer and Ranier Wolf for sharing their unpublished results. We are also very grateful to Kathy Miller for her collaboration in the microinjection experiments. Finally, we thank Gert Weil for her skilful drawings.

REFERENCES

- AGRELL, I. (1964). Natural division synchrony and mitotic gradients in metazoan tissues. In *Synchrony in Cell Division and Growth* (ed. E. Zeuthen). New York: Interscience.
- AUFDERHEIDE, K. J., FRANKEL, J. & WILLIAMS, N. E. (1980). Formation and positioning of surface-related structures in protozoa. *Microbiol. Rev.* **44**, 252-302.
- BULL, A. L. (1966). Bicaudal, a genetic factor which affects the polarity of the embryo in *Drosophila melanogaster*. *J. exp. Zool.* **161**, 221-242.
- BURGOYNE, L. A., WAGAR, M. A. & ATKINSON, M. R. (1970). Calcium dependent priming of DNA synthesis in isolated rat liver nuclei. *Biochem. Biophys. Res. Commun.* **39**, 254-259.
- CHAN, L. N. & GEHRING, W. (1971). Determination of blastoderm cells in *Drosophila melanogaster*. *Proc. natn. Acad. Sci. U.S.A.* **68**, 2217-2221.
- EDE, D. A. & COUNCE, S. J. (1956). A cinematographic study of the embryology of *Drosophila melanogaster*. *Wilhelm Roux Arch. EntwMech. Org.* **148**, 402-415.

- ELGIN, S. C. R. & MILLER, D. W. (1978). Mass rearing of flies and mass production and harvesting of embryos. In *The Genetics and Biology of Drosophila*, vol. 2a (ed. M. Ashburner & T. R. F. Wright), pp. 112–120. London, New York, San Francisco: Academic Press.
- FULLILOVE, S. L. & JACOBSON, A. G. (1971). Nuclear elongation and cytokinesis in *Drosophila montana*. *Devl Biol.* **26**, 560–577.
- GERHART, J., UBBELS, G., BLACK, S., HARA, K. & KIRSCHNER, M. (1981). A reinvestigation of the role of the grey crescent in axis formation in *Xenopus laevis*. *Nature, Lond.* **292**, 511–516.
- HEUSER, J. E. & KIRSCHNER, M. W. (1980). Filament organization revealed in platinum replicas of freeze-dried cytoskeletons. *J. Cell Biol.* **86**, 212–234.
- HUETTNER, A. F. (1933). Continuity of the centrioles in *Drosophila melanogaster*. *Z. Zellforsch mikrosk. Anat.* **19**, 119–134.
- ILLMENSEE, K. (1973). The potentialities of transplanted early gastrula nuclei of *Drosophila melanogaster*. Production of their imago descendants by germ-line transplantation. *Wilhelm Roux Arch. EntwMech. Org.* **171**, 331–343.
- ILLMENSEE, K. (1978). *Drosophila* chimeras and the problem of determination. In *Genetic Mosaics and Cell Differentiation* (ed. W. J. Gehring), vol. 9, pp. 51–69. Berlin, Heidelberg, New York: Springer-Verlag.
- KALTHOFF, K. (1979). Analysis of a morphogenetic determinant in an insect embryo (*Smittia* spec., chironomidae, diptera). In *Determinants of Spatial Organisation, 37th Symp., Soc. Develop. Biol.* (ed. S. Subtelny & I. R. Konigsberg), pp. 97–126. New York: Academic Press.
- KALTHOFF, K., HANEL, P. & ZISSLER, D. (1977). A morphogenetic determinant in the anterior pole of an insect egg (*Smittia* spec., chironomidae, diptera): localization by combined centrifugation and ultraviolet irradiation. *Devl Biol.* **55**, 285–305.
- KAUFFMAN, S. (1975). Control circuits for determination and transdetermination: interpreting positional information in a binary epigenetic code. In *Cell Patterning Ciba Fdn Symp.*, no. 29 (new series), pp. 201–221. Amsterdam: Elsevier.
- KAUFFMAN, S. A. (1980). Heterotopic transplantation in the syncytial blastoderm of *Drosophila*: evidence for anterior and posterior nuclear commitments. *Wilhelm Roux Arch. EntwMech. Org.* **189**, 135–145.
- KAUFFMAN, S. A. (1981). Pattern formation in the *Drosophila* embryo. *Phil. Trans. R. Soc. Lond. B* **295**, 567–594.
- KINSEY, J. D. (1967). Studies on an embryonic lethal hybrid in *Drosophila*. *J. Embryol. exp. Morph.* **17**, 405–423.
- LAMB, M. M. & LAIRD, C. D. (1976). Increase in nuclear poly(A)-containing RNA at syncytial blastoderm in *Drosophila melanogaster* embryos. *Devl Biol.* **52**, 31–42.
- LAWRENCE, P. A. (1981). The cellular basis of segmentation in insects. *Cell* **26**, 3–10.
- LIMBOURG, B. & ZALOKAR, M. (1973). Permeabilization of *Drosophila* eggs. *Devl Biol.* **35**, 382–387.
- LOHS-SCHARDIN, M., CREMER, C. & NUSSLEIN-VOLHARD, C. (1979). A fate map for the larval epidermis of *Drosophila melanogaster*: localized cuticle defects following irradiation of the blastoderm with an ultraviolet laser microbeam. *Devl Biol.* **73**, 239–255.
- MAHOWALD, A. P. (1963). Electron microscopy of the formation of the cellular blastoderm in *Drosophila melanogaster*. *Expl Cell Res.* **32**, 457–468.
- MCKNIGHT, S. L. & MILLER, O. L. JR (1976). Ultrastructural patterns of RNA synthesis during early embryogenesis of *Drosophila melanogaster*. *Cell* **8**, 305–319.
- MEINHARDT, H. (1977). A model of pattern formation in insect embryogenesis. *J. Cell Sci.* **23**, 117–139.
- MIYAMOTO, D. M. & VAN DER MEER, J. M. (1982). Early egg contractions and patterned parasychronous cleavage in a living insect egg. *Wilhelm Roux Arch. EntwMech. Org.* **191**, 95–102.
- NEWMAN, S. M. JR & SCHUBIGER, G. (1980). A morphological and developmental study of *Drosophila* embryos ligated during nuclear multiplication. *Devl Biol.* **79**, 128–138.
- NUSSLEIN-VOLHARD, C. (1979). Maternal effect mutations that alter the spatial coordinates of the embryo of *Drosophila melanogaster*. In *Determinants of Spatial Organisation* (ed. S. Subtelny & I. R. Konigsberg), pp. 185–211. New York: Academic Press.
- NUSSLEIN-VOLHARD, C., LOHS-SCHARDIN, M., SANDER, K. & CREMER, C. (1980). A dorsoventral shift of embryonic primordia in a new maternal-effect mutant of *Drosophila*. *Nature, Lond.* **283**, 474–476.

- OKADA, M., KLEINMAN, I. A. & SCHNEIDERMAN, H. A. (1974). Chimeric *Drosophila* adults produced by transplantation of nuclei into specific regions of fertilized eggs. *Devl Biol.* **39**, 286–294.
- OKADA, M., KOMATSU, H. & OKUMURA, M. (1980). Behavior of interphase embryonic nuclei transplanted in nuclear multiplication stage embryos of *Drosophila melanogaster*. *Dev. Growth & Differ.* **22**, 599–610.
- POULSON, D. F. (1950). Histogenesis, organogenesis, and differentiation in the embryo of *Drosophila melanogaster meigen*. In *Biology of Drosophila* (ed. M. Demerec), pp. 168–274. New York: John Wiley and Sons. Reprinted in 1965, New York, London: Hafner.
- RABINOWITZ, M. (1941a). Studies on the cytology and early embryology of the egg of *Drosophila melanogaster*. *J. Morph.* **69**, 1–49.
- RABINOWITZ, M. (1941b). Yolk nuclei in the egg of *Drosophila melanogaster*. *Anat. Rec.* **81** (suppl. 2), 80–81.
- REBHUN, L. I. (1972). Polarized intracellular particle transport: saltatory movements and cytoplasmic streaming. *Int. Rev. Cytol.* **32**, 93–137.
- RICKOLL, W. L. (1976). Cytoplasmic continuity between embryonic cells and the primitive yolk sac during early gastrulation in *Drosophila melanogaster*. *Devl Biol.* **49**, 304–310.
- RICKOLL, W. L. (1977). Analysis of morphogenesis in normal and mutant embryos of *Drosophila melanogaster*. Ph.D. dissertation, Duke University.
- RICKOLL, W. L. & COUNCE, S. J. (1980). Morphogenesis in the embryo of *Drosophila melanogaster* – germ band extension. *Wilhelm Roux Arch. EntwMech. Org.* **188**, 163–178.
- SANDER, K. (1975). Pattern specification in the insect embryo. In *Cell Patterning, Ciba Fdn Symp.*, no. 29 (new series), pp. 241–263. Amsterdam: Elsevier.
- SANDER, K. (1976). Specification of the basic body pattern in insect embryogenesis. *Adv. Insect Physiol.* **12**, 125–238.
- SANDER, K. (1981). Pattern generation and pattern conservation in insect ontogenesis – problems, data and models. In *Progress in Developmental Biology* (ed. H. W. Sauer), pp. 101–119. Stuttgart: Gustav Fischer Verlag.
- SCHLIWA, A. M., VAN BLERKOM, J. & PORTER, K. R. (1981). Stabilization of the cytoplasmic ground substance in detergent-opened cells and a structural and biochemical analysis of its composition. *Proc. natn. Acad. Sci. U.S.A.* **78**, 4329–4333.
- SCHUBIGER, G., MOSELEY, R. C. & WOOD, W. J. (1977). Interactions of different egg parts in determination of various body regions in *Drosophila melanogaster*. *Proc. natn. Acad. Sci. U.S.A.* **74**, 2050–2053.
- SCHUBIGER, G. & WOOD, W. J. (1977). Determination during early embryogenesis in *Drosophila melanogaster*. *Am. Zool.* **17**, 565–576.
- SINHA, B. J. & PELLEGRINI, M. (1982). Genomic clones coding for some of the initial genes expressed during *Drosophila* development. *Proc. natn. Acad. Sci. U.S.A.* **79**, 7351–7355.
- SONNENBLICK, B. P. (1950). The early embryology of *Drosophila melanogaster*. In *Biology of Drosophila* (ed. M. Demerec), pp. 62–167. New York: John Wiley and Sons. Reprinted in 1965, New York and London: Hafner.
- SWANSON, M. M. & POODRY, C. A. (1980). Pole cell formation in *Drosophila melanogaster*. *Devl Biol.* **75**, 419–430.
- TURNER, F. R. & MAHOWALD, A. P. (1976). Scanning electron microscopy of *Drosophila* embryogenesis. I. The structure of the egg envelope and the formation of the cellular blastoderm. *Devl Biol.* **50**, 95–108.
- TURNER, F. R. & MAHOWALD, A. P. (1977). Scanning electron microscopy of *Drosophila melanogaster* embryogenesis. II. Gastrulation and segmentation. *Devl Biol.* **57**, 403–416.
- VAN DER MEER, J. M., KEMMNER, W. & MIYAMOTO, D. M. (1982). Mitotic waves and embryonic pattern formation: no correlation in *Callosobruchus* (Coleoptera). *Wilhelm Roux Arch. EntwMech. Org.* **191**, 355–365.
- VOGEL, O. (1977). Regionalisation of segment-forming capacities during early embryogenesis in *Drosophila melanogaster*. *Wilhelm Roux Arch. EntwMech. Org.* **182**, 9–32.
- WARN, R. M. & MEGRATH, R. (1982). Observations by a novel method of surface changes during the syncytial blastoderm stage of the *Drosophila* embryo. *Devl Biol.* **89**, 540–548.
- WILSON, J. C. (1970). Analysis of pre-blastoderm cytoplasmic and nuclear movements in *Drosophila montana*. M.A. thesis, University of Texas at Austin.

- WOLF, R. (1978). The cytaster, a colchicine-sensitive migration organelle of cleavage nuclei in an insect egg. *Devl Biol.* **62**, 464–472.
- WOLF, R. (1983). Migration and division of cleavage nuclei in the gall midge *Wachtliella persicariae*. III. Experimental alteration of the cleavage pattern. *Wilhelm Roux Arch. EntwMech. Org.* (in press).
- WOLPERT, L. (1969). Positional information and the spatial pattern of cellular differentiation. *J. theor. Biol.* **25**, 1–47.
- ZALOKAR, M. (1976). Autoradiographic study of protein and RNA formation during early development of *Drosophila* eggs. *Devl Biol.* **49**, 425–437.
- ZALOKAR, M. & ERK, I. (1976). Division and migration of nuclei during early embryogenesis of *Drosophila melanogaster*. *J. Microbiol. Cell.* **25**, 97–106.

(Received 27 September 1982)